Exploring the Earth

NORSAR Scientific Report No.1-2014

Semiannual Technical Summary

1 January – 30 June 2014

Tormod Kværna (Ed.)

Kjeller, December 2014

NORSAR

Table of Contents

1 Summary

This report provides summary information on operation and maintenance (O&M) activities at the Norwegian National Data Center (NOR-NDC) for CTBT verification during the period 1 January – 30 June 2014, as well as scientific and technical contributions relevant to verification in a broad sense. The O&M activities, including operation of monitoring stations and transmission links within Norway and to Vienna, Austria are being funded jointly by the CTBTO/PTS and the Norwegian Government, with the understanding that the funding of O&M activities for primary stations in the International Monitoring System (IMS) will gradually be transferred to the CTBTO/PTS. The O&M statistics presented in this report maintain consistency with long-standing reporting practices. Research activities described in this report are mainly funded by the Norwegian Government, with other sponsors acknowledged where appropriate.

A summary of the activities at NOR-NDC relating to field installations, data acquisition, data forwarding and processing during the reporting period is provided in chapters 2 – 4 of this report. Norway contributes data from two primary seismic arrays: the Norwegian Seismic Array NOA (IMS code PS27) and the Arctic Regional Seismic Array ARCES (IMS code PS28), one auxiliary seismic array on Spitsbergen (SPITS, IMS code AS72), and one auxiliary three-component station at Jan Mayen (JMIC, IMS code AS73). In addition, NORSAR provides data from one infrasound array in northern Norway (IMS code IS37), and one radionuclide monitoring station on Spitsbergen (IMS code RN49). These data are provided to the International Data Centre (IDC) in Vienna via the Global Communications Infrastructure (GCI).

This report presents operational statistics for NOA, ARCES, SPITS, JMIC and IS37, as well as for additional seismic stations which through cooperative agreements with institutions in the host countries provide continuous data to the NOR-NDC. These additional stations include the Finnish Regional Seismic Array (FINES, IMS code PS17) and the Hagfors array in Sweden (HFS, IMS code AS101). Operational statistics for the reestablished NORES array and two other three-component stations operated by NORSAR are also provided. These two stations are Åknes (AKN) and TROLL in Antarctica.

All Norwegian IMS stations, the NOA and the ARCES seismic arrays (PS27 and PS28, respectively), the radionuclide station at Spitsbergen (RN49), the auxiliary seismic stations on Spitsbergen (AS72) and Jan Mayen (AS73), as well as the infrasound array at Bardufoss (IS37) are certified by the CTBTO/PTS. Provided that adequate funding continues to be made available (from the CTBTO/PTS and the Norwegian Ministry of Foreign Affairs), we envisage continuing the provision of data from these and other Norwegian IMS-designated stations in accordance with current procedures. As part of NORSAR's obsolescence management, a recapitalization plan for PS27 and PS28 was submitted to CTBTO/PTS in October 2008, with the purpose of preventing severe degradation of the stations due to lack of spare parts. The recapitalization of PS27 was concluded in 2012. In parallel the recapitalization of P28 has started with development and testing of particular equipment for PS28, like a central timing system and a hybrid sensor for surface vaults.

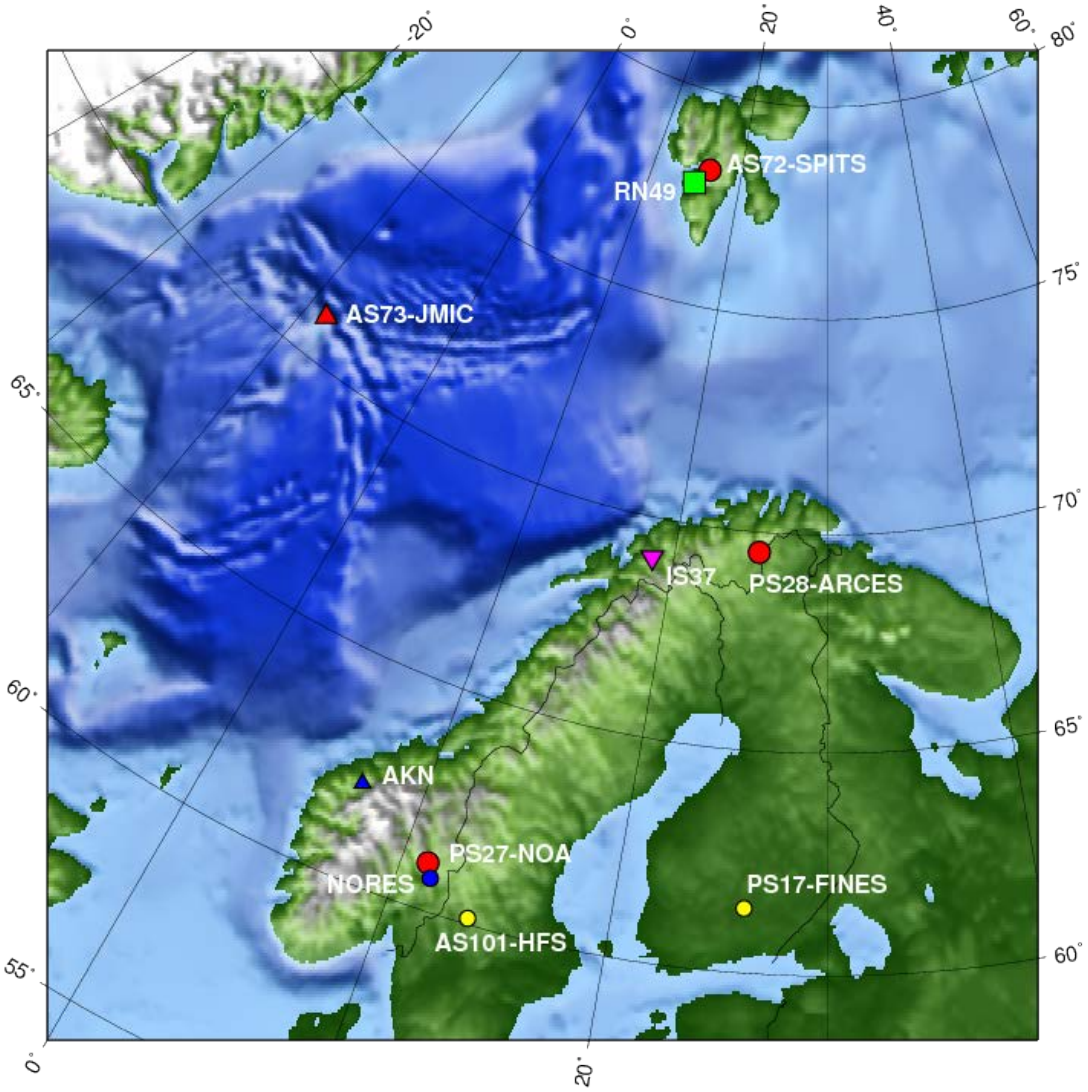

Fig. 1.1 *Locations of stations covered in this report (except TROLL in Antarctica, see Figure. 3.5.1). Norwegian seismic IMS stations are shown in red. Other Norwegian seismic stations are shown by blue symbols. Contributing IMS seismic stations in other countries are yellow. Circles indicate seismic arrays and triangles indicate single 3-component seismic stations. The IMS infrasound station IS37 is shown by a purple inverted triangle, and the IMS radionuclide station RN49 is shown by a green square.*

Three scientific and technical contributions presented in chapter 6 of this report are provided as follows:

Section 6.1 describes the results from an experiment involving the inclusion of the Eskdalemuir array (EKA) in Scotland in the automatic regional array processing system at NORSAR. The main purpose of the experiment was to assess the extent to which the processing and analysis of seismic events in the North Sea could be improved by such an augmentation of the monitoring network. For a 10-month period we ran an experimental processing system which included EKA and compared the results with the regular NORSAR processing over the same time period. The main conclusions are as follows:

- EKA is an excellent regional array, and inclusion of EKA in the NORSAR GBF processing works very well. EKA detections have been automatically associated with many seismic events already detected by the regular GBF processing during the time period.

- With EKA included, the NORSAR GBF detection list contains many small events in the North Sea region currently not being analyzed interactively at NORSAR. Thus, the inclusion of EKA would contribute to a more complete reviewed NORSAR regional bulletin.

- Addition of EKA gives a much improved azimuthal coverage for detected events, thus providing more accurate event locations. Furthermore, the array beams formed with EKA data give significant SNR improvements, thus enabling more precise phase arrival time estimates.

There are still some remaining improvements that could be considered. Thus, the EKA array data is currently processed using a generic recipe. Improved performance can be achieved by conducting a tuning study. The automatically calculated magnitudes at EKA have not yet been calibrated, and this obviously needs to be done. There might also be a need for considering Lg blockage across the Viking Graben when forming the generalized beams. Such blocking features occur also in other areas covered by the NORSAR regional processing, and should be considered there as well.

Section 6.2 presents the technical details of the modernized large-aperture NOA (NORSAR) array, and an evaluation of its performance as compared with the old system. The modernization, completed in July 2012, included new acquisition computers, modified pit boxes, new digitizers and new sensors. Güralp CMG_DM24S3AM acquisition modules were installed at all 42 sites of the array. For seismic sensors, also Güralp was chosen. Based on careful analysis of noise conditions and the need to have good monitoring capability of both regional high-frequency/low-magnitude events as well as global low-frequency/high-magnitude earthquakes, a so-called hybrid instrument response was designed for the new broadband sensors. The hybrid response is proportional to velocity for frequencies from 0.005Hz to about 0.2 Hz and for frequencies between 3 and 20 Hz. In the intermediate range the response is proportional to acceleration. The seven vault sites of NOA have been equipped with the 3-component sensor (CMG-3T Hybrid 360s – 50Hz) and the 35 borehole sites have been equipped with the vertical-component sensor (CMG-3V Hybrid 120s – 50 Hz).

All 42 sites of upgraded NOA array now contain broadband sensors, as compared with 7 sites for the old system. Consequently, significant improvements in processing of surface waves are demonstrated. For short-period signals, the excellent performance for processing of teleseismic signals is continued.

Section 6.3 considers infrasound propagation modelling. Results from a classical ray-tracing program are compared with results produced by the reflectivity method. The reflectivity method is applied widely by the seismological community to generate synthetic seismograms for elastic waves propagating in a stratified earth. For infrasound however, there is little previous work on comparing ray-tracing and the reflectivity method for modelling the propagation of observed infrasound signals.

We apply a ray-tracing engine and a reflectivity code to the atmospheric conditions along the great circle path which connects the Drevja accidental explosion in Nordland, northern Norway, on December 17, 2013 and the IS37 infrasound array station near Bardufoss, Troms, northern Norway. The modelling results are compared with the observed signals recorded at the array.

By applying reflectivity modelling, we can avoid some limitations of conventional ray-tracing, e.g., we can get better head wave representation and less pronounced shadow zones. This is illustrated in our Drevja explosion example: the reflectivity method predicts a phase arriving at the station after turning only once in the stratosphere, while ray tracing does not predict this phase (which is observed in the recorded signals).

There are seismic modelling codes which model anisotropic velocity, and we intend to test these out for infrasound propagation. We foresee to more accurately model wind effects, hence avoiding disadvantages appearing due to the $c_{effective}$ approximation that we had to apply in the reflectivity modelling described in the current work.

T. Kværna

2 Operation of International Monitoring System (IMS) Stations in Norway

2.1 PS27 — Primary Seismic Station NOA

The mission-capable data statistics were 100.000%, as compared to 99.998%for the previous reporting period. The net instrument availability was 98.598%

There were no outages of all subarrays at the same time in the reporting period.

Monthly uptimes for the NORSAR on-line data recording task, taking into account all factors (field installations, transmissions line, data center operation) affecting this task were as follows:

	Mission Capable	Net instrument availability
January 2014:	100.000	97.484
February 2014:	100.000	99.177
March 2014:	100.000	99.966
April 2014:	100.000	99.895
May 2014:	100.000	98.251
June 2014:	100.000	96.815

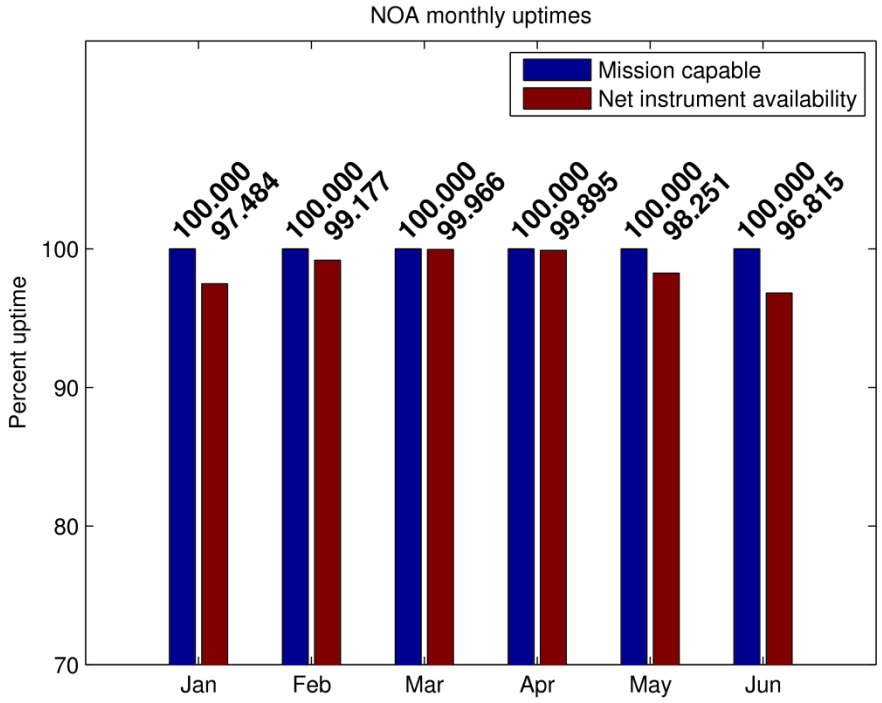

Fig. 2.1.1 Monthly uptimes for NOA for the period January - June 2014.

B. Paulsen

2.1.1 NOA event detection operation

In Table 2.1.1 some monthly statistics of the Detection and Event Processor operation are given. The table lists the total number of detections (DPX) triggered by the on-line detector, the total number of detections processed by the automatic event processor (EPX) and the total number of events accepted after analyst review (teleseismic phases, core phases and total).

	Total DPX	Total EPX	Accepted events P-phases	Core Phases	Sum	Daily average
Jan 14	7346	778	256	43	299	9.6
Feb	7588	929	257	47	304	10.9
Mar	6134	826	261	83	344	11.1
Apr	5862	854	250	124	374	12.5
May	4451	856	270	100	370	11.9
Jun	5210	911	278	163	441	14.7
	36591	5154	1572	560	2132	11.8

Table 2.1.1. Detection and event processor statistics, 1 January – 30 June 2014.

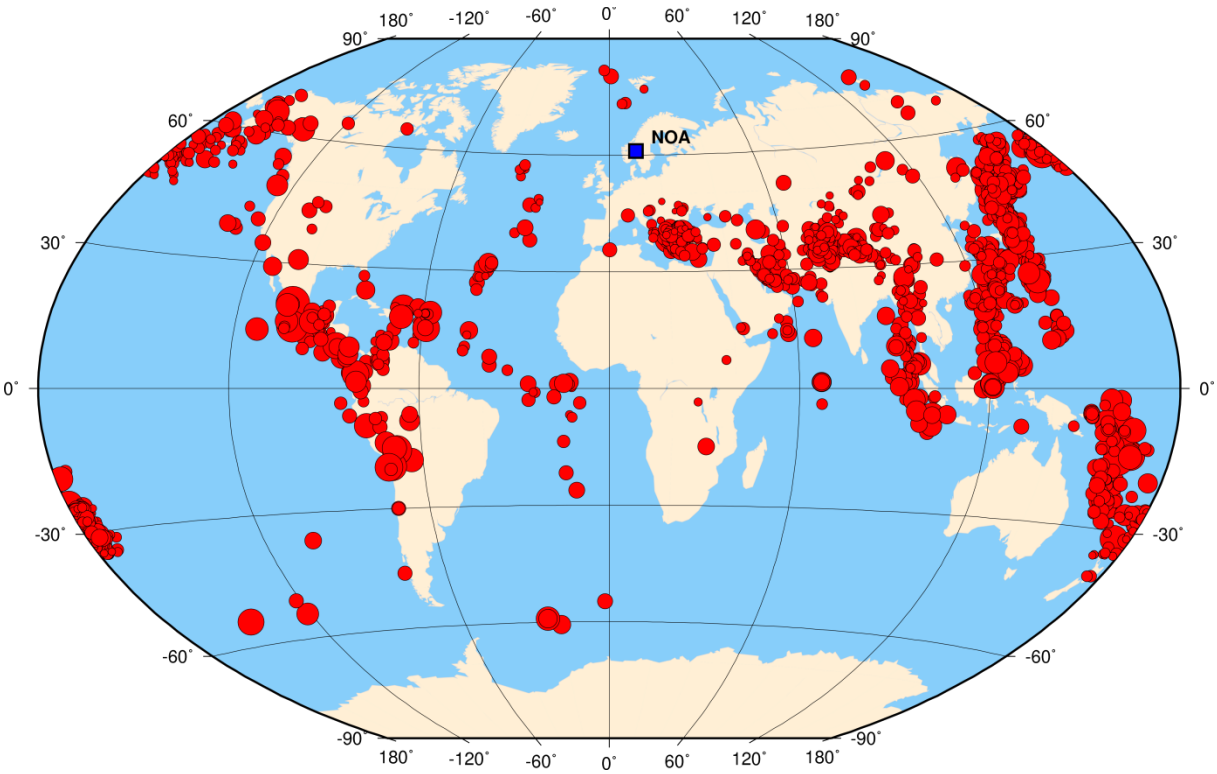

Fig. 2.1.2 Distribution of events in NORSAR's teleseismic reviewed bulletin for the time interval 1 January - 30 June 2014. Event symbols are scaled proportionally to event magnitude. The location of NOA is noted with a blue square. All locations are based on phase interpretation and inversion of slowness and backazimuth into a location, using the NOA array alone.

NOA detections

The number of detections (phases) reported by the NORSAR detector during day 001, 2014, through day 181, 2014, was 36,591, giving an average of 202 detections per processed day (181 days processed).

B. Paulsen
U. Baadshaug

2.2 PS28 — Primary Seismic Station ARCES

The mission-capable data statistics were 99.968%, as compared to 99.986% for the previous reporting period. The net instrument availability was 88.820%.
Monthly uptimes for the ARCES on-line data recording task, taking into account all factors (field installations, transmission lines, data center operation) affecting this task were as follows:

	Mission Capable	Net instrument availability
January 2014:	99.832	88.703
February 2014:	100.000	88.889
March 2014:	100.000	88.889
April 2014:	99.979	88.870
May 2014:	99.997	88.887
June 2014:	100.000	88.679

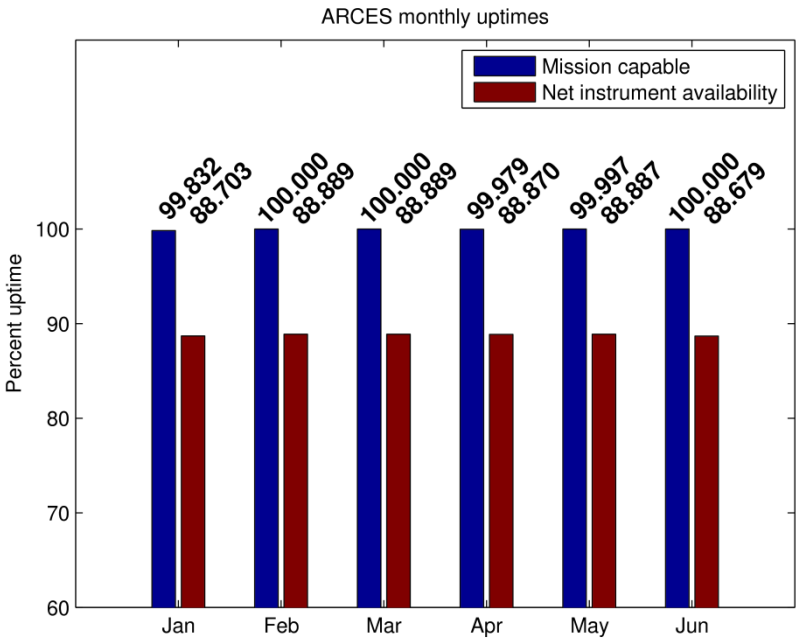

Fig. 2.2.1 Monthly uptimes for ARCES for the period January - June 2014.

B. Paulsen

2.2.1 Event detection operation

ARCES detections

The number of detections (phases) reported during day 001, 2014, through day 181, 2014, was 182,276, giving an average of 1007 detections per processed day (181 days processed).

Events automatically located by ARCES

During days 001, 2014, through day 181, 2014, 9,194 local and regional events were located by ARCES, based on automatic association of P- and S-type arrivals. This gives an average of 50.8 events per processed day (181 days processed). 78% of these events are within 300 km, and 94% of these events are within 1000 km.

U. Baadshaug

2.3 AS72 — Auxiliary Seismic Station on Spitsbergen

The mission-capable data for the period were 97.226%, as compared to 98.356% for the previous reporting period. The net instrument availability was 93.969%.

Monthly uptimes for the Spitsbergen on-line data recording task, taking into account all factors (field installations, transmissions line, data center operation) affecting this task were as follows:

	Mission Capable	Net instrument availability
January 2014:	99.973	90.978
February 2014:	99.971	95.203
March 2014:	83.547	79.053
April 2014:	99.974	99.956
May 2014:	99.931	99.924
June 2014:	99.961	98.701

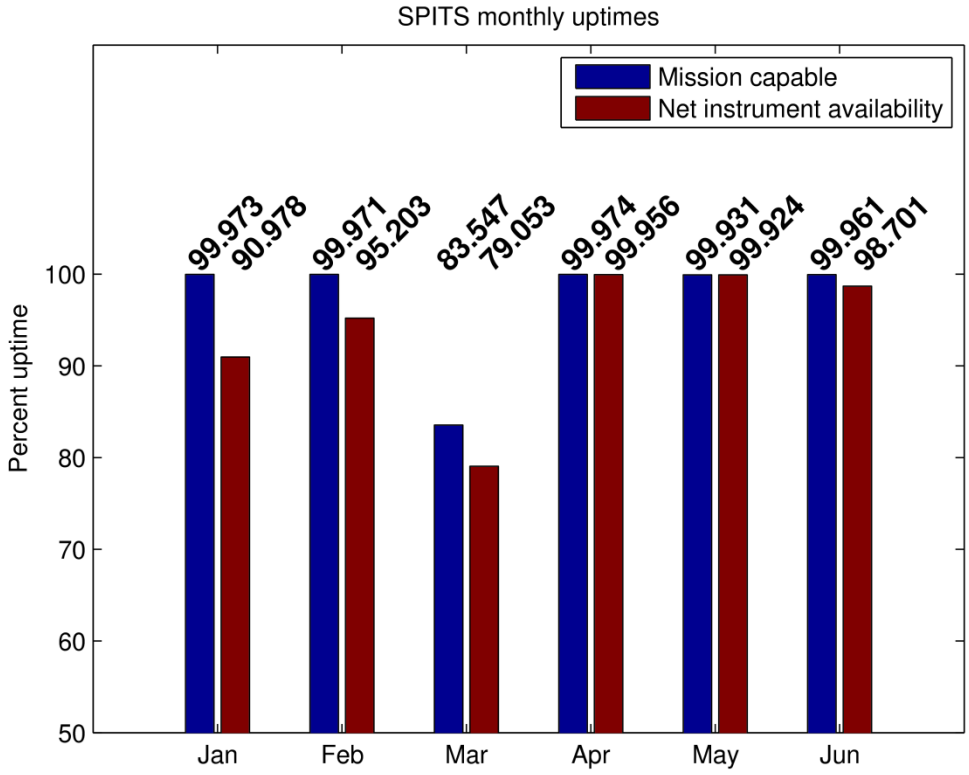

Fig. 2.3.1 Monthly uptimes for SPITS for the period January - June 2014.

The low availability in March is caused by a power outage at the station between 7 and 12 March 2014 when both the Whispergen generators and the windmill failed and had to be repaired.

B. Paulsen

2.3.1 Event detection operation

Spitsbergen array detections

The number of detections (phases) reported from day 001, 2014, through day 181, 2014, was 352,488, giving an average of 1,839 detections per processed day (177 days processed).

Events automatically located by the Spitsbergen array

During days 001, 2014, through day 181, 2014, 26,272 local and regional events were located by the Spitsbergen array, based on automatic association of P- and S-type arrivals. This gives an average of 148.4 events per processed day (177 days processed). 83% of these events are within 300 km, and 92% of these events are within 1000 km.

U. Baadshaug

2.4 AS73 — Auxiliary Seismic Station at Jan Mayen

The IMS auxiliary seismic network includes a three-component station on the Norwegian island of Jan Mayen. The station location given in the protocol to the Comprehensive Nuclear- Test-Ban Treaty is 70.9°N, 8.7°W.

The University of Bergen has operated a seismic station at this location since 1970. A so-called Parent Network Station Assessment for AS73 was completed in April 2002. A vault at a new location (71.0°N, 8.5°W) was prepared in early 2003, after its location had been approved by the CTBTO PrepCom. New equipment was installed in this vault in October 2003, as a cooperative effort between NORSAR and the CTBTO/PTS. Continuous data from this station are being transmitted to the NDC at Kjeller via a satellite link installed in April 2000. Data are also made available to the University of Bergen.

The station was certified by the CTBTO/PTS on 12 June 2006.
Monthly uptimes for the Jan Mayen on-line data recording task, taking into account all factors (field installations, transmissions line, data center operation) affecting this task were as follows:

	Mission Capable	Net instrument availability
January 2014:	99.878	99.882
February 2014:	99.956	99.959
March 2014:	99.914	99.918
April 2014:	99.723	99.728
May 2014:	99.974	99.974
June 2014:	99.860	99.860

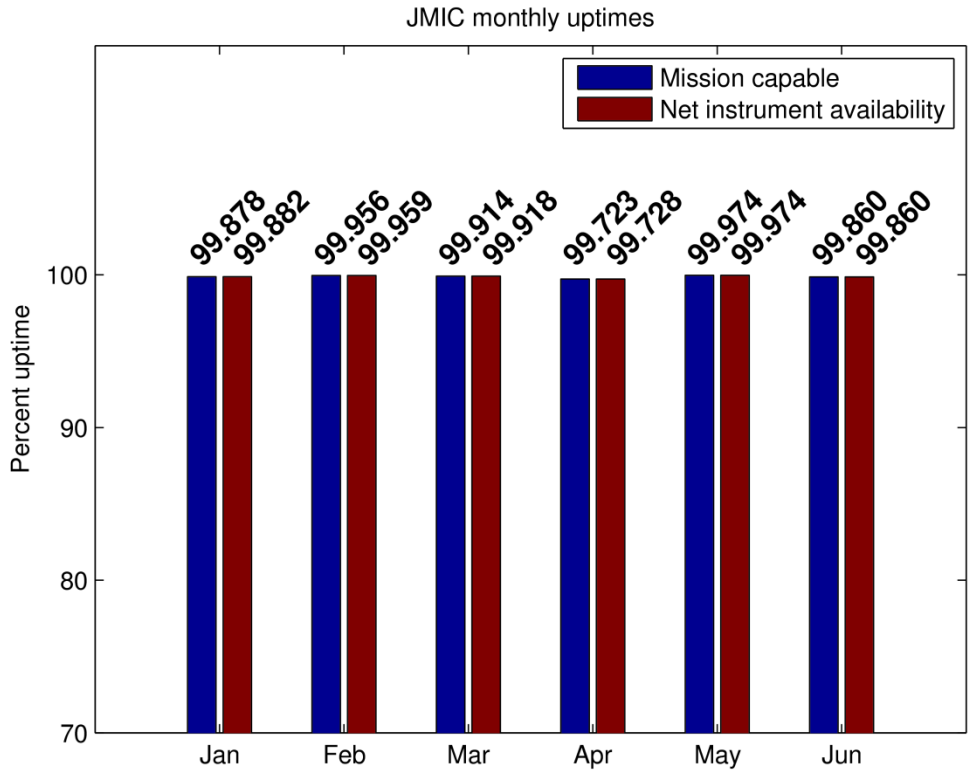

Fig. 2.4.1 Monthly uptimes for JMIC for the period January - June 2014.

B. Paulsen

2.5 IS37 — Infrasound Station at Bardufoss

Monthly uptimes for the IS37 on-line data recording task, taking into account all factors (field installations, transmissions line, data center operation) affecting this task were as follows:

	Mission Capable	Net instrument availability
January 2014:	100.000	100.000
February 2014:	100.000	100.000
March 2014:	100.000	99.996
April 2014:	100.000	100.000
May 2014:	100.000	100.000
June 2014:	99.998	99.995

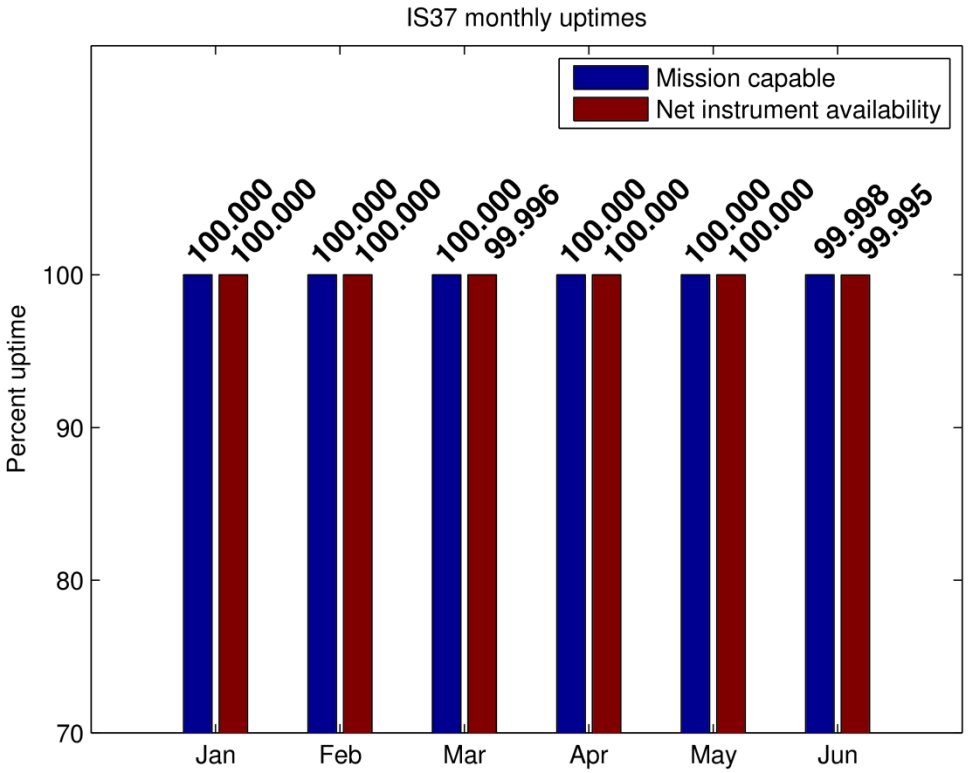

Fig. 2.5.1 Monthly uptimes for IS37 for the period January - June 2014.

U. Baadshaug

2.6 RN49 — Radionuclide Station on Spitsbergen

The IMS radionuclide network includes a station on the island of Spitsbergen. This station was selected to be among those IMS radionuclide stations that will monitor for the presence of relevant noble gases upon entry into force of the CTBT.

A site survey for this station was carried out in August of 1999 by NORSAR, in cooperation with the Norwegian Radiation Protection Authority. The site survey report to the PTS contained a recommendation to establish this station at Platåberget, near Longyearbyen. The infrastructure for housing the station equipment was established in early 2001, and a noble gas detection system, based on the Swedish "SAUNA" design, was installed at this site in May 2001, as part of CTBTO PrepCom's noble gas experiment. A particulate station ("ARAME" design) was installed at the same location in September 2001. A certification visit to the particulate station took place in October 2002, and the particulate station was certified on 10 June 2003. Both systems underwent substantial upgrades in May/June 2006. The noble gas system was certified on 21 December 2012. The equipment at RN49 is being maintained and operated under a contract with the CTBTO/PTS.

S. Mykkeltveit

3 Contributing Regional Arrays and Three-Component Stations

3.1 NORES

The NORES array went out of operation on 11 June 2002, when lightning destroyed the station electronics. In December 2011 the array was rebuilt and again became operational in an experimental mode where the 9 inner sites were instrumented with three-component sensors.

Monthly uptimes for the NORES on-line data recording task, taking into account all factors (field installations, transmission lines, data center operation) affecting this task are given in the following table:

	Data availability
January 2014:	100.000
February 2014:	100.000
March 2014:	100.000
April 2014:	100.000
May 2014:	98.631
June 2014:	100.000

B. Paulsen

3.2 Hagfors (IMS Station AS101)

Data from the Hagfors array are made available continuously to NORSAR through a cooperative agreement with Swedish authorities.

The mission-capable data statistics were 98.130%, as compared to 98.749% for the previous reporting period. The net instrument availability was 98.525%.

Monthly uptimes for the Hagfors on-line data recording task, taking into account all factors (field installations, transmission lines, data center operation) affecting this task were as follows:

	Mission Capable	Net instrument availability
January 2014:	99.998	99.999
February 2014:	99.999	100.000
March 2014:	99.151	99.198
April 2014:	99.997	99.999
May 2014:	91.875	94.034
June 2014:	97.760	97.921

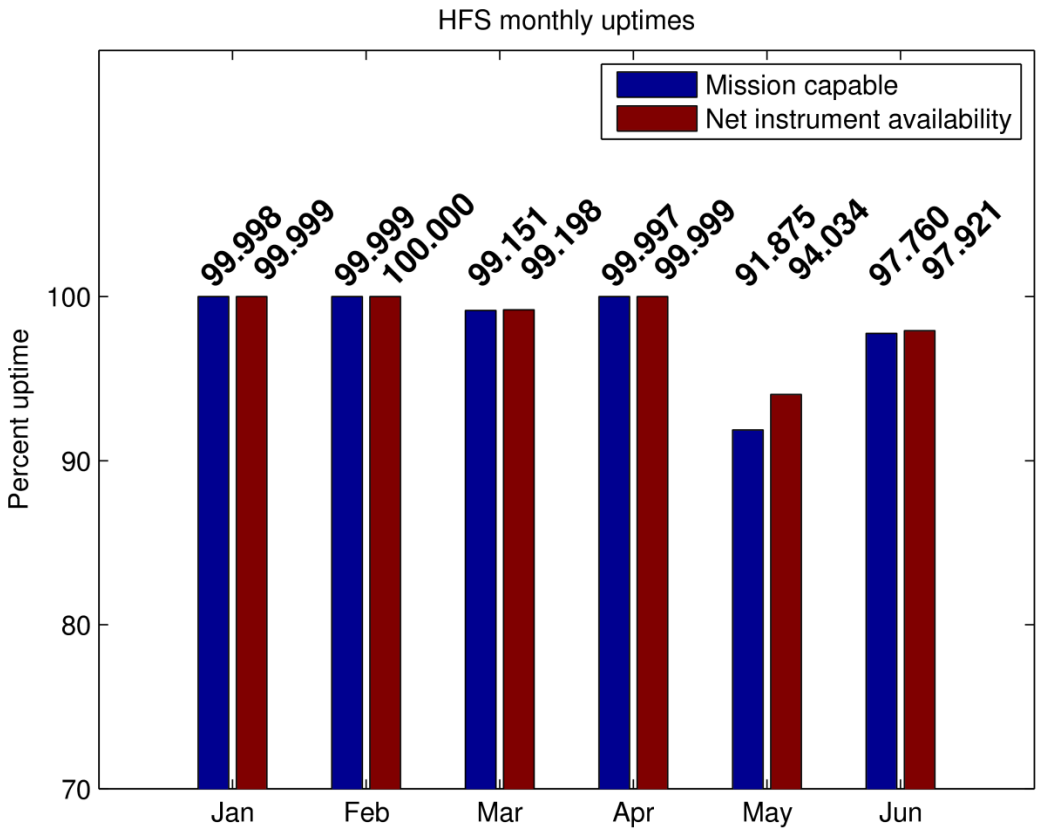

Fig. 3.2.1 Monthly uptimes for HFS for the period January - June 2014.

B. Paulsen

3.2.1 Hagfors event detection operation

Hagfors array detections

The number of detections (phases) reported from day 001, 2014, through day 181, 2014, was 149,219, giving an average of 834 detections per processed day (179 days processed).

Events automatically located by the Hagfors array

During days 001, 2014, through day 181, 2014, 7,405 local and regional events were located by the Hagfors array, based on automatic association of P- and S-type arrivals. This gives an average of 41.4 events per processed day (179 days processed). 79% of these events are within 300 km, and 94% of these events are within 1000 km.

U. Baadshaug

3.3 FINES (IMS Station PS17)

Data from the FINES array are made available continuously to NORSAR through a cooperative agreement with Finnish authorities.

The mission-capable data statistics were 99.067%, as compared to 99.833% for the previous reporting period. The net instrument availability was 97.296%.

Monthly uptimes for the FINES on-line data recording task, taking into account all factors (field installations, transmissions line, data center operation) affecting this task were as follows:

	Mission Capable	Net instrument availability
January 2014:	99.964	99.366
February 2014:	100.000	100.000
March 2014:	100.000	100.000
April 2014:	100.000	100.000
May 2014:	98.262	98.064
June 2014:	99.992	99.992

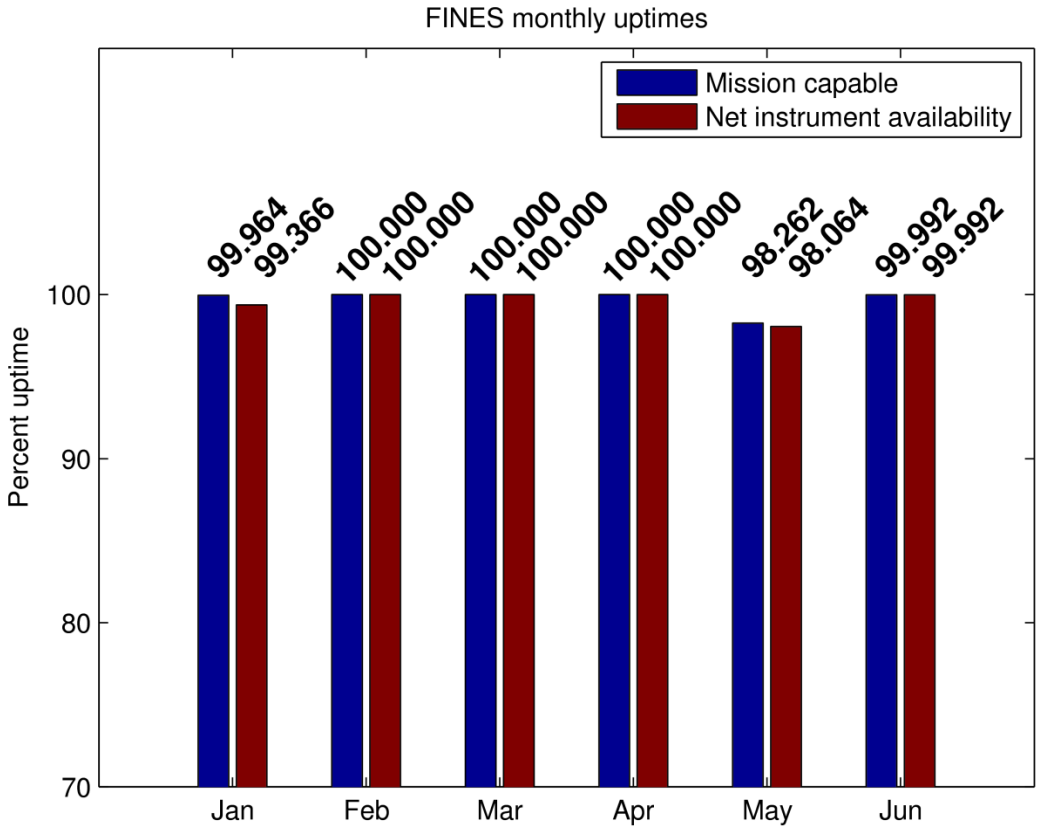

Fig. 3.3.1 Monthly uptimes for FINES for the period January - June 2014.

B. Paulsen

3.3.1 FINES event detection operation

FINES detections

The number of detections (phases) reported during day 001, 2014, through day 181, 2014, was 44,401, giving an average of 245 detections per processed day (181 days processed).

Events automatically located by FINES

During days 001, 2014, through day 181, 2014, 1,824 local and regional events were located by FINES, based on automatic association of P- and S-type arrivals. This gives an average of 10.1 events per processed day (181 days processed). 84% of these events are within 300 km, and 94% of these events are within 1000 km.

U. Baadshaug

3.4 Åknes (AKN)

The seismic broadband station AKN was installed in October 2009 on top of the unstable rock slope site Åknes, Møre og Romsdal. Its primary purpose is the monitoring of local seismic activity related to the movement of the slope, but due to the relatively low ambient noise conditions it also provides excellent data for local, regional and global seismic events. The station has been sending continuous real-time data (200 Hz sampling rate) to NORSAR since 27 October 2009. On 17 January 2013 we added a 40 Hz data tap in order to facilitate data distribution to the seismological community.

Monthly uptimes for the AKN on-line data recording task, taking into account all factors (field installations, transmission lines, data center operation) affecting this task are given in the following table:

	Data availability
January 2014:	100.000
February 2014:	100.000
March 2014:	99.997
April 2014:	100.000
May 2014:	100.000
June 2014:	100.000

U. Baadshaug

3.5 TROLL, Antarctica

The seismic station at the Norwegian Research Base Troll in Dronning Maud Land, Antarctica, became operational and started sending continuous data to NORSAR on 5 February 2012. On 4 February 2013 the Q330HR digitizer gain was increased by a factor of 20, and on 9 February 2013, the TROLL station was upgraded with additional thermal insulation. An additional low-gain data stream with a sampling rate of 40 Hz was retained by using the auxiliary 24-bit input and a gain factor of 1.

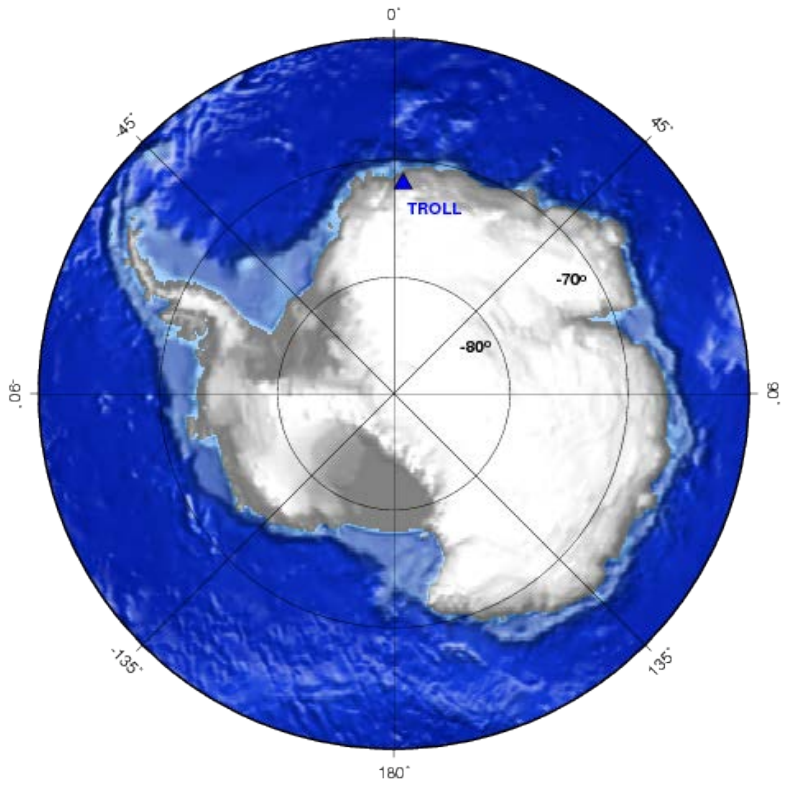

Fig. 3.5.1
Location of the 3-component seismic station TROLL in Antarctica.

Monthly uptimes for the TROLL on-line data recording task, taking into account all factors (field installations, transmission lines, data center operation) affecting this task are given in the following table:

	Data availability
January 2014:	100.000
February 2014:	100.000
March 2014:	100.000
April 2014:	100.000
May 2014:	100.000
June 2014:	100.000

U. Baadshaug

3.6 Regional Monitoring System Operation and Analysis

The Regional Monitoring System (RMS) was installed at NORSAR in December 1989 and has been operated from 1 January 1990 for automatic processing of data from ARCES and NORES. Several updates have been installed, and the current version of RMS that accepts data from an arbitrary number of arrays and single 3-component stations and has also the capability of locating events at teleseismic distances. All array data available at the NDC is being automatically processed and all data, including 3-component single stations are made available to the analyst for review of events.

3.6.1 Phase and event statistics

Table 3.6.1 gives a summary of phase detections and events declared by RMS. From top to bottom the table gives the total number of detections by the RMS, the number of detections that are associated with events automatically declared by the RMS, the number of detections that are not associated with any events, the number of events automatically declared by the RMS, and finally the total number of events worked on interactively (in accordance with criteria that vary over time; see below) and defined by the analyst.

New criteria for interactive event analysis were introduced from 1 January 1994. Since that date, only regional events in areas of special interest (e.g., Spitsbergen, since it is necessary to acquire new knowledge in this region) or other significant events (e.g., felt earthquakes and large industrial explosions) were thoroughly analyzed. Teleseismic events of special interest are also analyzed.

The GBF program is used as a pre-processor to RMS, and only phases associated with selected events in northern Europe are considered in the automatic RMS phase association. All detections, however, are still available to the analysts and can be added manually during analysis.

	Jan 14	Feb 14	Mar 14	Apr 14	May 14	Jun 14	Total
Phase detections	163683	116272	126870	156116	141394	147868	852203
- Associated phases	7415	6225	7087	7281	8132	7178	43318
- Unassociated phases	156268	110047	119783	148835	133262	140690	808885
Events automatically declared by RMS	1413	1021	1222	1283	1286	1260	7485
No. of events defined by the analyst	47	35	43	45	55	40	265

Table 3.6.1. RMS phase detections and event summary 1 January - 30 June 2014.

U. Baadshaug
B. Paulsen

4 The Norwegian National Data Center and Field Activities

4.1 NOR-NDC Activities

NORSAR functions as the Norwegian National Data Center (NOR-NDC) for CTBT verification. Six monitoring stations, comprising altogether 87 seismic and infrasound waveform sensor sites plus radionuclide monitoring equipment, are located on Norwegian territory as part of the IMS, as described elsewhere in this report. The four seismic IMS stations are all in operation today, and all of them are currently providing data to the CTBTO/PTS on a regular basis. PS27, PS28, AS72, AS73, RN49 and IS37are all certified. Data recorded by the Norwegian stations are being transmitted in real time to the NOR-NDC, and provided to the IDC through the Global Communications Infrastructure (GCI). Norway is connected to the GCI with an MPLS link to Vienna.

Operating the Norwegian IMS stations continues to require significant efforts by personnel both at the NOR-NDC and in the field. Strictly defined procedures as well as increased emphasis on regularity of data recording and timely data transmission to the IDC in Vienna have led to increased reporting activities and implementation of new procedures for the NOR-NDC. The NOR-NDC carries out all the technical tasks required in support of Norway's treaty obligations. NORSAR will also carry out assessments of events of special interest, and advise the Norwegian authorities in technical matters relating to treaty compliance. A challenge for the NOR-NDC is to carry 40 years' experience over to the next generation of personnel.

4.1.1 Verification functions; information received from the IDC

After the CTBT enters into force, the IDC will provide data for a large number of events each day, but will not assess whether any of them are likely to be nuclear explosions. Such assessments will be the task of the States Parties, and it is important to develop the necessary national expertise in the participating countries. An important task for the NOR-NDC will thus be to make independent assessments of events of particular interest to Norway, and to communicate the results of these analyses to the Norwegian Ministry of Foreign Affairs.

4.1.2 Monitoring the Arctic region

Norway will have monitoring stations of key importance for covering the Arctic, including Novaya Zemlya, and Norwegian experts have a unique competence in assessing events in this region. On several occasions in the past, seismic events near Novaya Zemlya have caused political concern, and NORSAR specialists have contributed to clarifying these issues.

4.1.3 International cooperation

After entry into force of the treaty, a number of countries are expected to establish national expertise to contribute to the treaty verification on a global basis. Norwegian experts have been in contact with experts from several countries with the aim of establishing bilateral or multilateral cooperation in this field.

4.1.4 NORSAR event processing

The automatic routine processing of NORSAR events as described in NORSAR Sci. Rep. No. 2-93/94, has been running satisfactorily. The analyst tools for reviewing and updating the solutions have been continually modified to simplify operations and improve results. NORSAR is currently applying teleseismic detection and event processing using the large-aperture NOA array, as well as regional monitoring using the network of small-aperture arrays in Fennoscandia and adjacent areas.

4.1.5 Communication topology

Norway has implemented an independent subnetwork, which connects the IMS stations AS72, AS73, PS28, RN49 and IS37 operated by NORSAR to the GCI at the NOR-NDC. VSAT is used for communication for PS28 and AS73. VSAT antennas for 6 of the PS27 subarrays have been installed for intra-array communication. The seventh subarray is connected to the central recording facility via a leased land line. The central recording facility for PS27 is connected directly to the GCI (Basic Topology). All VSAT communication is functioning satisfactorily. Since 10 June 2005, AS72 and RN49 have been connected to the NOR-NDC through a VPN link. IS37 is also connected to the NOR-NDC through two redundant VPN links. One based on a WIFI Internet service, an one based on GSM service. The IS37 system for communication has proven to be very successful, with a lot of available capacity, and is a model for changing communication for PS27 and PS28.

J. Fyen

4.2 Status Report: Provision of Data from Norwegian Seismic IMS Stations to the IDC

4.2.1 Introduction

This contribution is a report for the period January – June 2014 on activities associated with provision of data from Norwegian seismic IMS stations to the International Data Centre (IDC) in Vienna. This report represents an update of contributions that can be found in previous editions of NORSAR's Semiannual Technical Summary. All four Norwegian seismic stations providing data to the IDC have been formally certified.

4.2.2 Norwegian IMS stations and communications arrangements

During the reporting interval, Norway has provided data to the IDC from the five stations shown in Fig. 4.2.1. PS27 — NOA is a 60 km aperture teleseismic array, comprising of 7 subarrays, each containing five vertical broadband sensors and one three-component hybrid broadband instrument. PS28 — ARCES is a 25-element regional array with an aperture of 3 km, whereas AS72 — Spitsbergen array (station code SPITS) has 9 elements within a 1-km aperture. AS73 — JMIC has a single three-component broadband instrument. IS37 is a 10-element infrasound array.

The intra-array communication for NOA utilizes a land line for subarray NC6 and VSAT links based on iDirect technology for the other 6 subarrays. The central recording facility for NOA is located at the Norwegian National Data Center (NOR-NDC).

Continuous ARCES data are transmitted from the ARCES site to the NOR-NDC using the same iDirect network as NOA.

Continuous SPITS data are transmitted to NOR-NDC via the central recording facility (CRF) for the SPITS array at the University Centre in Svalbard (UNIS). Data from the array elements to the CRF are transmitted via a 2.4 Ghz radio link (Wilan VIP-110). A 512 Kbps SHDSL link has been established between UNIS and NOR-NDC. Both AS72 and RN49 data are now transmitted to NOR-NDC over this link using VPN technology.

A minimum of 14-day station buffers have been established at the IS37, ARCES and SPITS sites and at all NOA subarray sites, as well as at the NOR-NDC for IS37, ARCES, SPITS and NOA. In addition, each individual site of the IS37, SPITS and NOA arrays has a 14-days buffer.

The NOA and ARCES arrays are primary stations in the IMS network, which implies that data from these stations are transmitted continuously to the receiving International Data Centre. Since October 1999, these data have been transmitted (from NOR-NDC) via the Global Communications Infrastructure (GCI) to the IDC in Vienna. Data from the auxiliary array station SPITS — AS72 have been sent in continuous mode to the IDC during the reporting period. AS73 — JMIC is an auxiliary station in the IMS, and also this station is transmitted in continuous mode to the IDC. In addition, continuous data from all three arrays are transmitted to the US_NDC under a bi-lateral agreement.

NORSAR also provides broadband data from Norwegian IMS stations to ORFEUS and IRIS.

4.2.3 Uptimes and data availability

Figs. 4.2.2, 4.2.3 and 4.2.4 show the monthly uptimes for the Norwegian IMS primary stations ARCES and NOA, and the IMS infrasound array IS37, respectively, for the reporting period given as the red (taller) bars in these figures. These barplots reflect the percentage of the waveform data that is available in the NOR-NDC data archives for these three arrays. The downtimes inferred from these figures thus represent the cumulative effect of field equipment outages, station site to NOR-NDC communication outage, and NOR-NDC data acquisition outages.

Figs. 4.2.2, 4.2.3 and 4.2.4 also give the data availability for these three stations as reported by the IDC in the IDC Station Status reports.

4.2.4 NOR-NDC automatic processing and data analysis

These tasks have proceeded in accordance with the descriptions given in Sci. Rep. No. 2-95/96 (Mykkeltveit and Baadshaug). For the reporting period NOR-NDC derived information on 264 events and submitted this information to the Finnish NDC as the NOR-NDC contribution to the Bulletin of seismic events in northern Europe. These events are plotted in Fig. 4.2.5.

4.2.5 Current developments and future plans

NOR-NDC is continuing the efforts towards improving and hardening all critical data acquisition and data forwarding hardware and software components, so as to meet the requirements related to operation of IMS stations.

The NOA array was formally certified by the PTS on 28 July 2000, and a contract with the PTS in Vienna currently provides partial funding for operation and maintenance of this station. The ARCES array was formally certified by the PTS on 8 November 2001, and a contract with the PTS is in place which also provides for partial funding of the operation and maintenance of this station. The operation of the two IMS auxiliary seismic stations on Norwegian territory (Spitsbergen and Jan Mayen) is funded by the Norwegian Ministry of Foreign Affairs. Provided that adequate funding continues to be made available (from the PTS and the Norwegian Ministry of Foreign Affairs), we envisage continuing the provision of data from all Norwegian seismic IMS stations without interruption to the IDC in Vienna.

The IS37 station was certified on 19 December 2013 and a contract with the PTS is in place for the operation and maintenance of this station.

The PS27 - NOA equipment was recapitalized during 2010-2012, and has been revalidated. The PS28 - ARCES equipment was acquired in 1999, and it is no longer possible to get spare digitizers. A recapitalization plan for the array was submitted to the PTS in October 2008, and development and testing of specific equipment for that array are ongoing.

U. Baadshaug
S. Mykkeltveit
J. Fyen

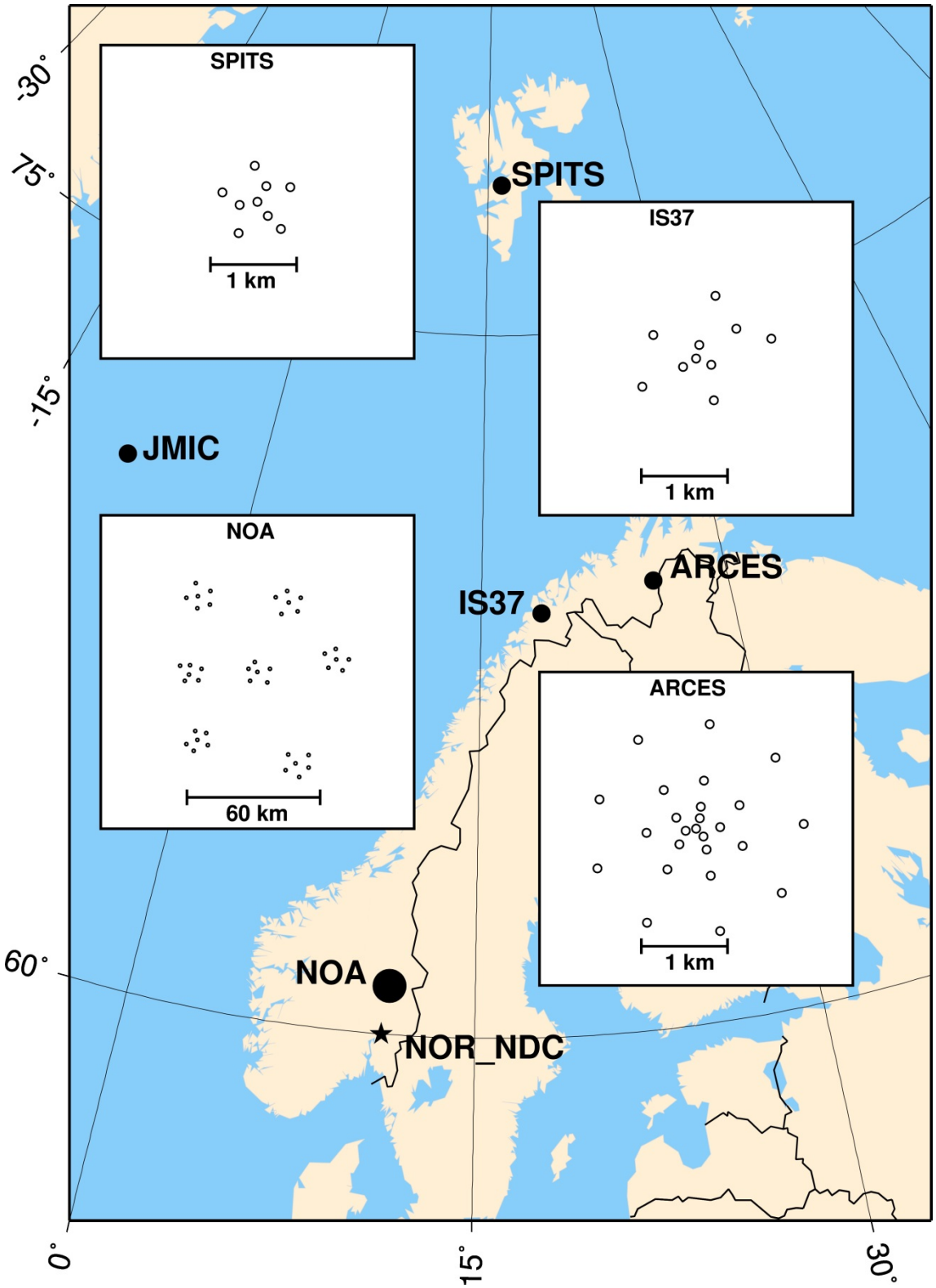

Fig. 4.2.1. The figure shows the locations and configurations of the three Norwegian seismic IMS array stations that provided data to the IDC during the period January - June 2014. The data from these stations and the JMIC three-component station are transmitted continuously and in real time to the Norwegian NDC (NOR-NDC). The stations NOA and ARCES are primary IMS stations, whereas SPITS and JMIC are auxiliary IMS stations. JMIC is a three-component station, the other stations are arrays. IS37 is an IMS infrasound station.

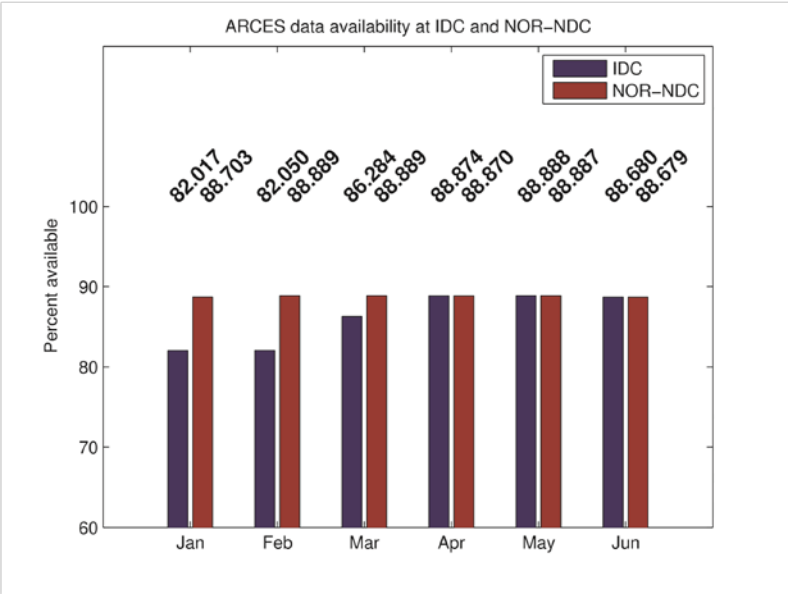

Fig. 4.2.2 The figure shows the monthly availability of ARCES array data for the period January – June 2014 at NOR-NDC and the IDC.

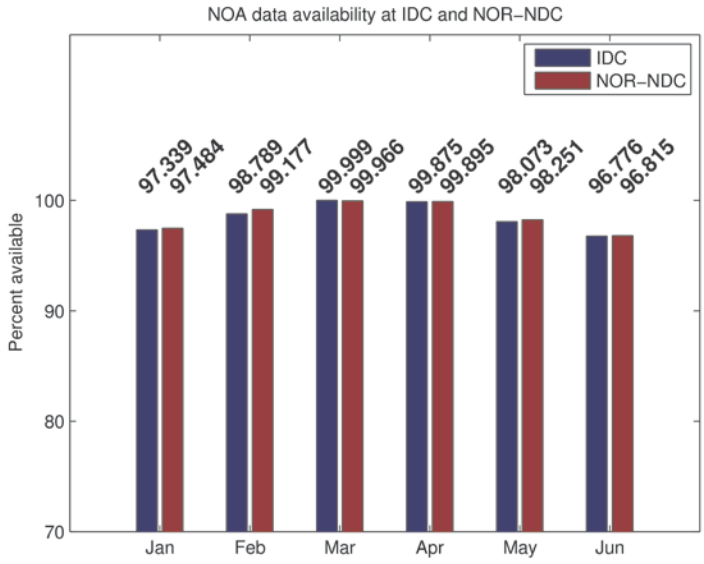

Fig. 4.2.3 The figure shows the monthly availability of NOA array data for the period January – June 2014 at NOR-NDC and the IDC.

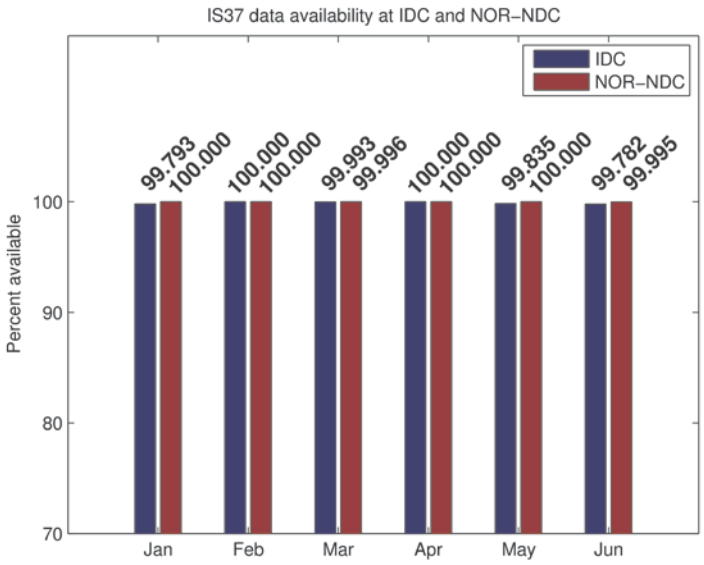

Fig. 4.2.4 The figure shows the monthly availability of IS37 infrasound array data for the period January – June 2014 at NOR-NDC and the IDC.

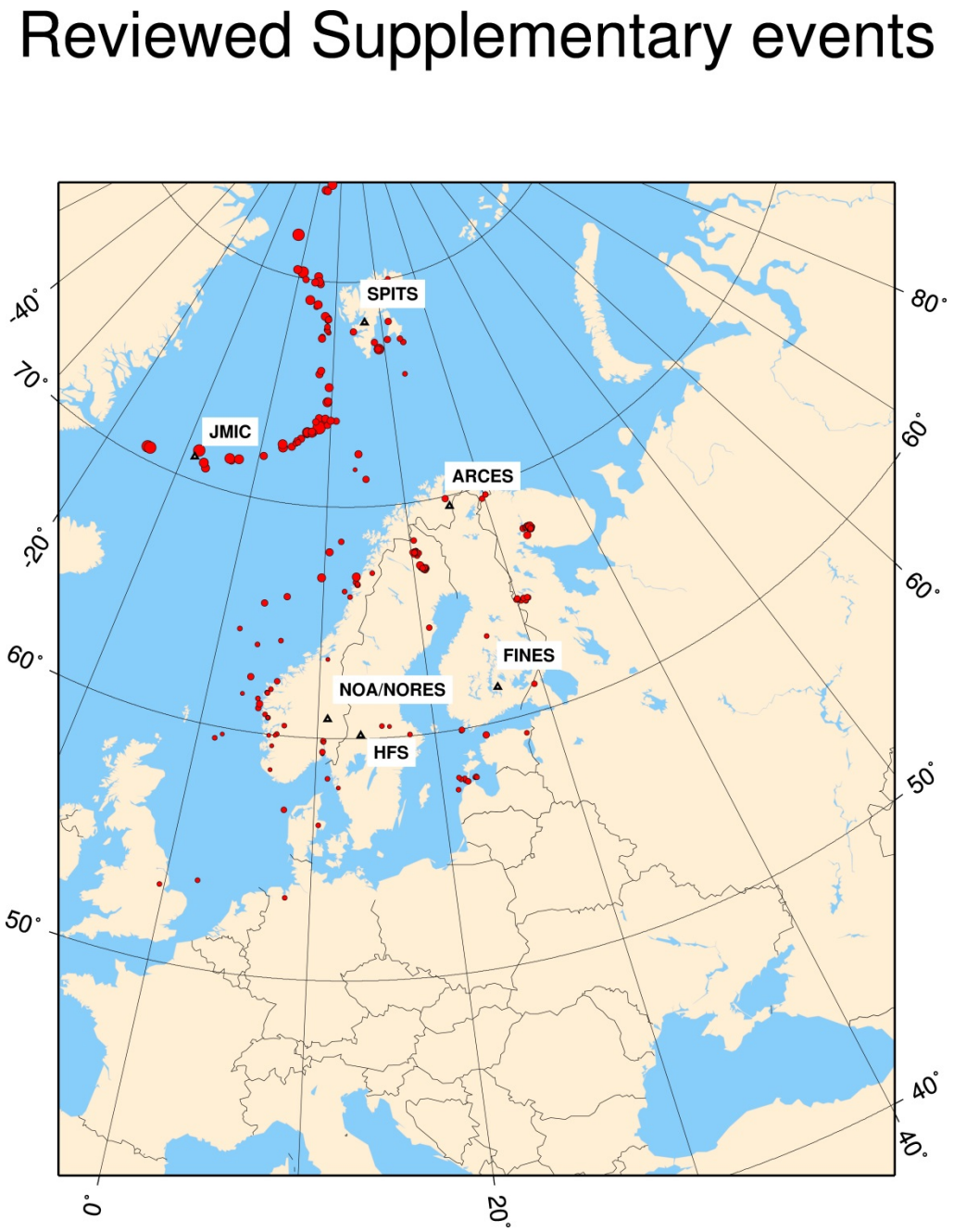

Fig. 4.2.5 The map shows the 264 events in and around Norway contributed by NOR-NDC during January - June 2014 to the Bulletin of seismic events in northern Europe compiled by the Finnish NDC. The map also shows the main seismic stations used in the data analysis to define these events.

4.3 Field Activities

The activities at the NORSAR Maintenance Center (NMC) at Hamar currently include work related to operation and maintenance of the following IMS seismic stations: the NOA teleseismic array (PS27), the ARCES array (PS28) and the Spitsbergen array (AS72). Some work has also been carried out in connection with the seismic station on Jan Mayen (AS73), the radionuclide station at Spitsbergen (RN49), and installation of the infrasound station IS37. NORSAR also acts as a consultant for the operation and maintenance of the Hagfors array in Sweden (AS101).

NORSAR carries out the field activities relating to IMS stations in a manner generally consistent with the requirements specified in the appropriate IMS Operational Manuals, which are currently being developed by Working Group B of the Preparatory Commission. For seismic stations these specifications are contained in the Operational Manual for Seismological Monitoring and the International Exchange of Seismological Data (CTBT/WGB/TL-11/2), currently available in a draft version.

All regular maintenance on the NORSAR field systems is conducted on a one-shift-per-day, five-day-per-week basis. The maintenance tasks include:

- Operating and maintaining the seismic sensors and the associated digitizers, authentication devices and other electronics components.
- Maintaining the power supply to the field sites, as well as backup power supplies.
- Operating and maintaining the VSATs, the data acquisition systems and the intra-array data transmission systems.
- Assisting the NDC in evaluating the data quality and making the necessary changes in gain settings, frequency response and other operating characteristics as required.
- Carrying out preventive, routine, and emergency maintenance to ensure that all field systems operate properly.
- Maintaining a computerized record of the utilization, status, and maintenance history of all site equipment.
- Providing appropriate security measures to protect against incidents such as intrusion, theft and vandalism at the field installations.

Details of the daily maintenance activities are kept locally. As part of its contract with CTBTO/PTS, NORSAR submits, when applicable, problem reports, outage notification reports and equipment status reports. The contents of these reports and the circumstances under which they will be submitted are specified in the draft Operational Manual.

P.W. Larsen
K.A. Løken

5 Documentation Developed

Clinton, J.F., M. Nettles, F. Walter, K. Anderson, T. Dahl-Jensen, D. Giardini, A. Govoni, W. Hanka, S. Lasocki, W.S. Lee, D. McCormack, S. Mykkeltveit, E. Stutzmann and S. Tsuboi. Seismic Network in Greenland Monitors Earth and Ice System. Eos Trans. AGU, **95**, no.2.

Gibbons, S.J. (2014). The Applicability of Incoherent Array Processing to IMS Seismic Arrays. Pure and Applied Geophysics, **171**, 377-394.

Holm, S. and S.P. Näsholm (2014). Comparison of Fractional Wave Equations for Power Law Attenuation in Ultrasound and Elastography. Ultrasound in Medicine and Biology, **40**, 695 – 703.

Näsholm, S.P., J. Schweitzer, T. Kværna and S.J. Gibbons (2014). Reflectivity versus ray-tracing in infrasound propagation modelling.
In: NORSAR Scientific Report **1-2014**, Semiannual Technical Summary,
1 January – 30 June 2014.

Oye, V., K. Iranpour, T. Kværna, S. Gibbons, L. Vedvik and H.H. Nielsen (2014). Migration-based Location Method Applied to a Perforation Shot Using LoFS Data at the Ekofisk Field, Norway. 76th EAGE Conference and Exhibition 2014, doi: 10.3997/2214-4609.20141436

Ringdal, F., T. Kværna and J. Schweitzer (2014). Experimental inclusion of the Eskdalemuir array in the automatic regional array processing system at NORSAR.
In: NORSAR Scientific Report **1-2014**, Semiannual Technical Summary,
1 January – 30 June 2014.

Roth, M., J. Schweitzer and J. Fyen (2014). The modernized large-aperture broadband array NOA.
In: NORSAR Scientific Report **1-2014**, Semiannual Technical Summary,
1 January – 30 June 2014.

6 Technical Reports / Papers Published

6.1 Experimental inclusion of the Eskdalemuir array in the automatic regional array processing system at NORSAR

6.1.1 Introduction

NORSAR has since 1991 carried out processing and analysis of seismic events in the European Arctic, using the regional array network in Fennoscandia and NW Russia. In previous Semiannual Technical Summaries, we have described the basic algorithms as well as a number of enhancements made to the regional processing at NORSAR over the years; see for example Kværna et al. (1999), Ringdal and Kværna (2004) and Schweitzer and Kværna (2006).

In summary, the regional processing comprises the following steps:

- Automatic single array processing, using a suite of bandpass filters in parallel and a beam deployment that covers both P and S type phases for the region of interest.
- An STA/LTA detector applied independently to each beam, with broadband f-k analysis for each detected phase in order to estimate azimuth and phase velocity.
- Single-array phase association for initial location of seismic events, and also for the purpose of chaining together phases belonging to the same event, so as to prepare for the subsequent multi-array processing.
- Multi-array event detection, using the Generalized Beamforming (GBF) approach (Ringdal and Kværna, 1989) to associate phases from all stations in the regional network and thereby provide automatic network location estimates for detected events in all of northern Europe. The resulting automatic event list is made available on the Internet (www.norsardata.no).
- Interactive analysis of selected events, resulting in a reviewed regional seismic bulletin, which includes hypocentral information, magnitudes and selected waveform plots. This reviewed bulletin is also available on the Internet.

The stations contributing to the automatic processing currently include the Fennoscandian seismic arrays (NORES, ARCES, NOA, HFS, FINES) as well as the Spitsbergen and Apatity arrays. A typical example of the automatic processing results as provided on Internet is shown in Figure 6.1.1. In our subsequent interactive analysis we also make use of some of the three-component seismic stations in the region to improve the event location accuracy.

Experience over the past several years has demonstrated that the automated event list generated by the GBF procedure is nearly “complete”, in the sense that it provides close to an exhaustive search of all possible phase combinations that could correspond to real events. The reviewed bulletin is much more selective, since our available resources allow a complete analysis of only a small subset of the seismic event candidates that are associated through the automatic algorithms. An important topic of current research is to develop methods to enable the analyst to easily select events from areas of particular interest, and focus on these events in the interactive analysis.

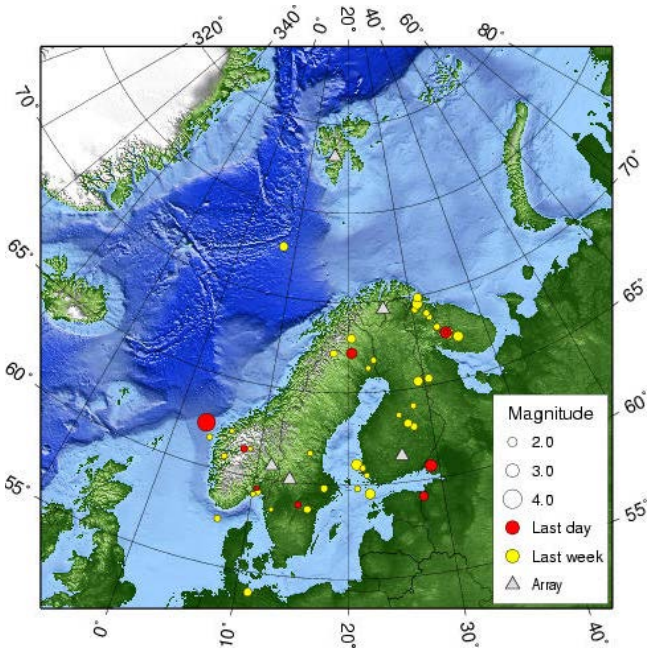

Origin time	Lat	Lon	Azres	Timres	Nph	Nst	Mag	Area
2014-290:08.08.10	60.71	29.14	4.91	1.71	6	3	2.53	BALTIC STATES-BELARUS-NW RUSSIA REGION
2014-290:03.39.47	67.70	34.31	6.18	2.29	4	2	1.12	BALTIC STATES-BELARUS-NW RUSSIA REGION
2014-289:22.43.46	62.27	3.33	6.77	2.85	13	7	3.73	MOERE SHELF
2014-289:17.03.08	67.19	20.49	6.34	1.51	7	6	2.18	CENTRAL NORBOTTEN SWEDEN
2014-289:16.52.57	61.39	8.23	8.17	2.11	5	3	1.40	OPPLAND-HEDMARK NORWAY
2014-289:13.00.40	58.83	14.85	10.53	2.53	4	3	1.50	EASTERN GOETALAND SWEDEN
2014-289:11.50.20	67.68	34.30	5.78	1.56	5	2	2.45	BALTIC STATES-BELARUS-NW RUSSIA REGION
2014-289:11.31.34	59.14	27.86	8.59	2.93	4	2	1.93	BALTIC STATES-BELARUS-NW RUSSIA REGION
2014-289:11.01.24	59.43	10.37	5.97	0.59	6	4	1.03	OSLO REGION NORWAY
2014-288:23.51.16	67.99	20.45	6.95	1.18	4	2	1.80	CENTRAL NORBOTTEN SWEDEN
2014-288:21.59.52	66.35	22.76	10.78	2.93	4	3	1.14	SWEDISH-FINISH BORDER ZONE
2014-288:15.53.40	61.57	4.16	12.47	2.96	5	3	1.28	NORTHERN NORTH SEA
2014-288:14.54.13	69.90	31.27	13.46	2.53	4	2	1.89	NORWAY-MURMANSK BORDER REGION
2014-288:14.17.50	58.42	12.17	4.22	1.66	6	3	1.02	VAERMLAND REGION SWEDEN
2014-288:13.17.17	57.45	7.06	11.28	3.17	8	3	1.49	EASTERN NORTH SEA
2014-288:11.05.14	68.10	33.26	3.05	0.85	4	3	1.47	BALTIC STATES-BELARUS-NW RUSSIA REGION
2014-288:11.02.23	59.79	17.43	7.05	1.52	10	4	1.63	VAESTMANLAND REGION SWEDEN
2014-288:10.01.23	65.40	30.60	5.77	3.79	6	4	1.79	FINLAND-KARELIA BORDER REGION
2014-288:09.50.49	67.29	35.86	6.51	1.05	4	3	2.20	BALTIC STATES-BELARUS-NW RUSSIA REGION
2014-288:08.04.24	62.18	6.43	5.97	1.06	5	3	1.03	SOGN-MOERE REGION NORWAY
2014-288:07.29.08	60.78	6.25	3.57	0.79	5	3	1.28	HARDANGER NORWAY
2014-288:03.35.24	67.70	34.31	8.80	2.25	4	3	1.70	BALTIC STATES-BELARUS-NW RUSSIA REGION
2014-288:02.43.35	67.70	34.83	9.71	2.29	6	2	1.52	BALTIC STATES-BELARUS-NW RUSSIA REGION
2014-288:00.24.27	69.57	31.02	5.09	1.14	4	3	2.13	NORWAY-MURMANSK BORDER REGION

Fig. 6.1.1 Example of the NORSAR on-line automatic GBF processing results that are made available on the Web. These solutions are not reviewed by an analyst, and should therefore be interpreted with caution. The network of seismic arrays used in this processing is marked by triangles.

6.1.2 Monitoring North Sea seismicity

One of the primary areas of interest for the regional processing at NORSAR is the North Sea region. The seismicity pattern of this region is well known, and it is illustrated in Figure 6.1.2, based on the ISC bulletin for the time period 2000 – 2014. We show the seismicity with three different magnitude constraints (M>2.5, M>3.0 and M>3.5) in order to minimize any possible bias due to geographical variations in the regional event detection capability.

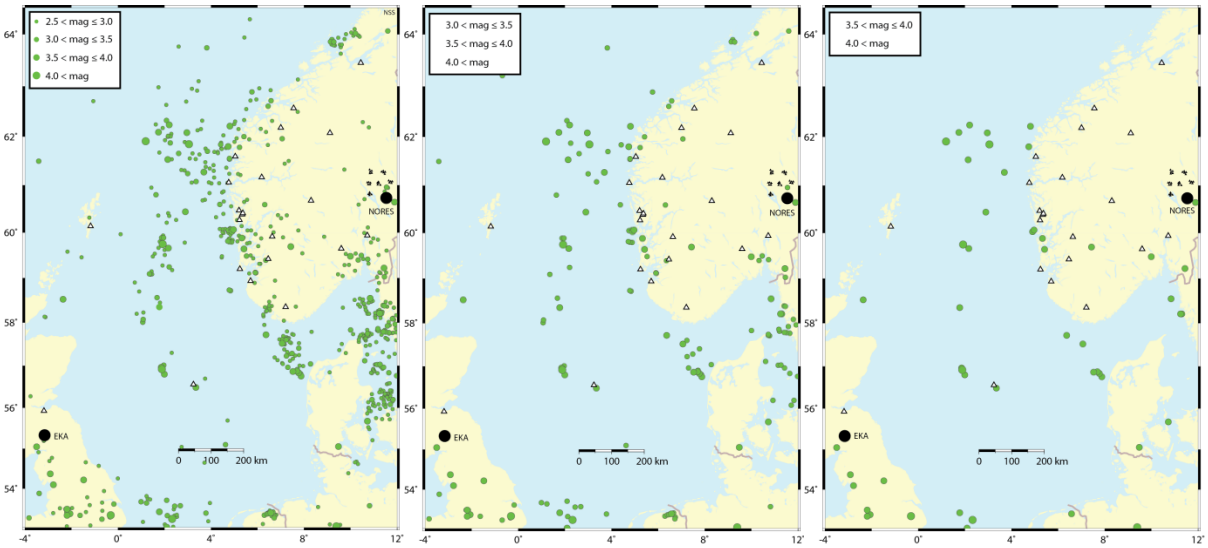

Fig. 6.1.2 Seismicity of the North Sea area as given in the ISC bulletin for the time period 2000 - 2014. The map shows all reported events with magnitude M restricted to a) M> 2.5, b) M>3.0 and c) M>3.5. The location of the two seismic arrays NORES (NRS) and EKA are labelled, and the stations of the Norwegian National Seismic Network (NNSN) are shown by black triangles.

From Figure 6.1.2 we can conclude that the seismic activity is not homogeneous in the general North Sea area. Most of the earthquakes occur near the west coast of Norway, with much lower seismic activity in the area near Britain. Some of the smaller events are likely explosions, but we are confident that all the events above M=3.5 are earthquakes. We are also confident that all seismic events above 3.5 in the region have been detected and included in the ISC bulletin.

An issue that must be considered with regard to NORSAR's regional monitoring of the North Sea is the location of the regional array network currently contributing to our processing. As can be seen from Figure 6.1.1, this network has a very poor azimuthal coverage of the North Sea region. A seismic array that might contribute to an improved coverage in this regard is the Eskdalemuir array (EKA) in Scotland, the location of which is indicated on Figure 6.1.2. The EKA array geometry is shown in Figure 6.1.3. The array is composed of two arms approximately at right angles, each arm being about 8 km long with seismometers at intervals of about 1 km. EKA has been in operation for more than 40 years, and has been designated as an auxiliary seismic station in the International Monitoring System for the Comprehensive Nuclear-Test-Ban Treaty. The excellent teleseismic detection capabilities of the array have been well documented over the years, and in addition, as we will document in this paper, the array is well suited for monitoring regional seismicity.

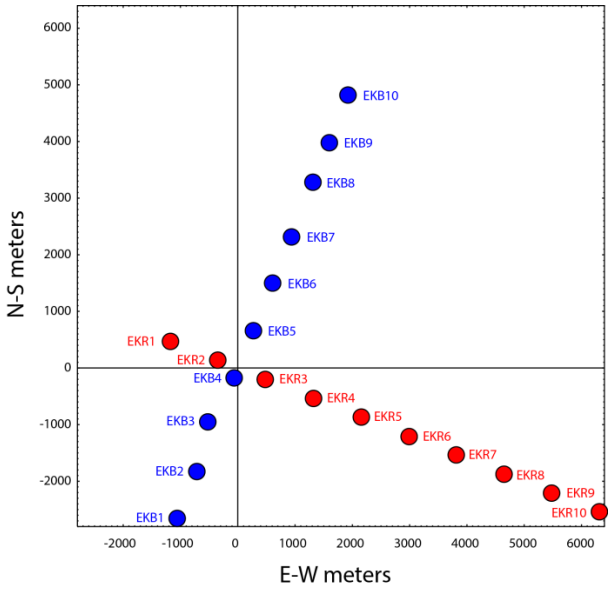

Fig. 6.1.3 Geometry of the Eskdalemuir seismic array (EKA) in Scotland.

6.1.3 Testing the NORSAR GBF with the inclusion of EKA array data

NORSAR has access to real-time EKA data, but until now these data have not been used in our automatic GBF analysis. In this paper we investigate the potential improvements obtained by including the EKA array in the automatic regional processing system, especially in connection with the monitoring of low-magnitude seismicity in the North Sea.

We have run experimental GBF network processing with inclusion of the EKA array since 1 December 2013, covering a period of approximately 10 months. This has been done in parallel to our regular GBF processing and has resulted in a comprehensive joint automatic seismic bulletin. An example of the result of this automatic processing for an event in the North Sea is shown in Figure 6.1.4.

```
EASTERN NORTH SEA
    Origin time        Lat      Lon    Azres  Timres  Wres  Nphase Ntot  Nsta Netmag
2014-084:18.19.55.0   57.09     7.28    8.04   3.21   5.22     8    14     4   1.65

Sta   Dist    Az    Ph     Time      Tres   Azim    Ares    Vel    Snr      Amp     Freq  Fkq Pol   Arid   Mag
NRS   474.6  213.0  Pn  18.21.01.5    0.7  208.9    -4.1    7.9    13.9     455.1  12.25   2       258383
NRS   474.6  213.0   p  18.21.09.4         206.8    -6.2    9.5     8.7     191.7   4.18   1       258386
NRS   474.6  213.0  Sn  18.21.51.3    2.3  193.1   -19.9    4.3     8.1     736.6   8.01   2  -3   258390  1.43
HFS   504.5  230.5  Pn  18.21.05.0    0.6  229.4    -1.1    8.2     5.8     312.2   8.00   2  -1   258384
HFS   504.5  230.5   p  18.21.11.8         227.2    -3.3    7.8     4.3     108.0   4.00   1       258385
HFS   504.5  230.5   p  18.21.15.8         223.4    -7.1    7.1     2.6     141.0  10.00   3       258387
HFS   504.5  230.5   p  18.21.19.3         228.8    -1.7    7.4     2.5      60.0  13.33   4       258388
HFS   504.5  230.5   s  18.21.52.2         225.5    -5.0    4.9     3.5     269.5   5.71   3   3   258393
HFS   504.5  230.5  Sn  18.21.58.1    2.9  235.0     4.5    4.6     4.5     252.0   4.11   3       258395  1.16
HFS   504.5  230.5  Lg  18.22.07.7  -11.4  238.4     7.9    3.8     2.7     280.4   4.28   3       258398  1.19
EKA   676.2   68.9  Pn  18.21.26.9    1.6   74.9     6.0    8.4     6.3      50.1   3.36   3   1   148300
EKA   676.2   68.9   p  18.21.27.0          74.5     5.6    8.2     6.3      50.1   3.36   3   1   148295
EKA   676.2   68.9  Sn  18.22.37.0    5.6   76.4     7.5    4.8     4.1      44.2   4.31   3   1   148305  2.32**
FIN  1172.2  254.0  Pn  18.22.26.2    0.7  240.7   -13.3    9.5     6.3     105.8   4.00   1   1   258392
```

Fig. 6.1.4 Example showing the results from the automatic GBF processing including the EKA array for a low-magnitude seismic event in the Eastern North Sea. Note that we have not yet included an appropriate calibration factor for EKA magnitudes, which currently are too high.

We have analyzed in some detail the EKA data for the event shown in Figure 6.1.4 in order to obtain a closer impression of the array capability. Figure 6.1.5 illustrates the gain in signal-to-noise ratio (SNR) from beamforming on the EKA array. The plot displays the P-beam (red) and the S-beam (blue) together with the individual seismic channels (black). The traces are filtered in the 2-4 Hz band. We note a significant improvement in SNR both for the P-beam and the S-beam, which means that these phases would be easily detected by automatic processing.

Figure 6.1.6 shows frequency-wavenumber analysis of the same event. The cross-like patterns of the two plots reflect the geometry of the array, but we note that both plots have clear peaks that turn out to correspond well with the event location. The estimated phase velocities in the two plots correspond to a Pn phase and an Sn phase, respectively, and the estimated azimuths for the two phases are mutually consistent (74.9 and 74.2 degrees). Thus the results from EKA array processing are very satisfactory.

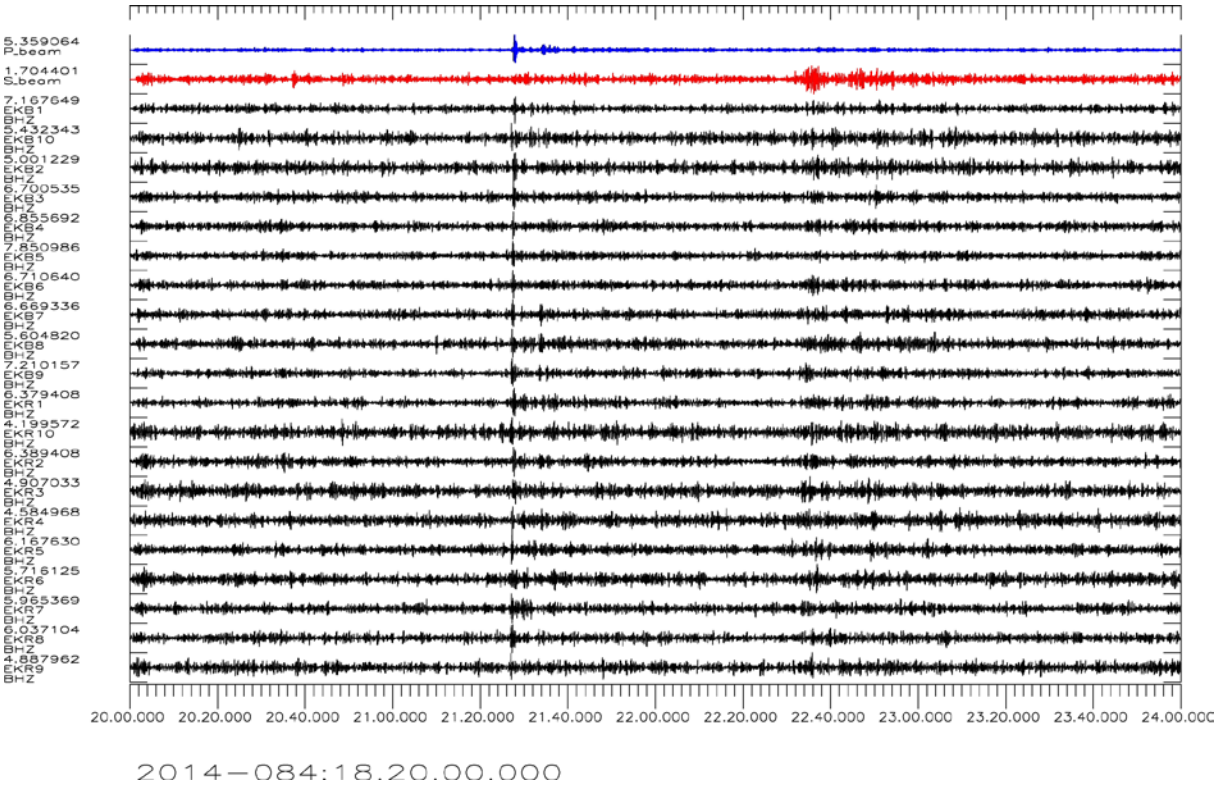

Fig. 6.1.5 Illustration of the gain in signal-to-noise ratio (SNR) from beamforming on the EKA array. The plot corresponds to the event shown in Figure 6.1.4, and displays the P-beam (red) and the S-beam (blue) together with the individual seismic channels (black). The traces are filtered in the 2-4 Hz band.

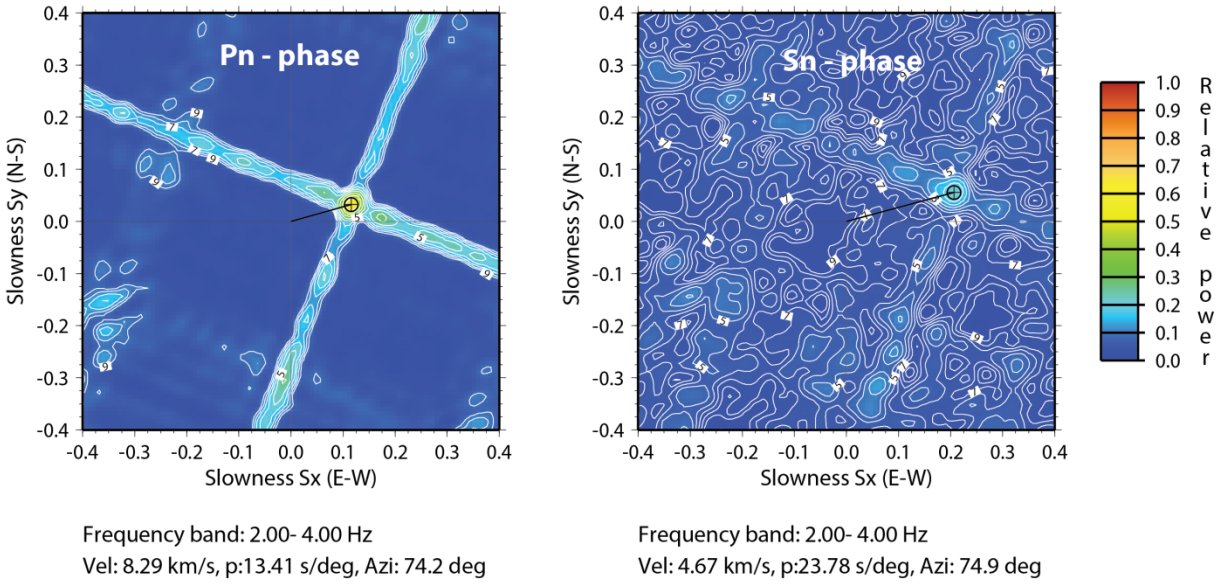

Fig. 6.1.6 Frequency-wavenumber analysis of the event shown in Figures 6.1.4 and 6.1.5. Note the excellent results for both the P-wave and S-wave, both with regard to phase velocity and azimuth.

Over the 10-month processing period with the EKA array, the GBF process has generated many thousand event candidates. Without analyzing the results in detail, we have noticed that a large number of acceptable events are within local distance from the array, and are detected and located by a standard EKA P and S phase combination. These local events are of little interest for our regional processing. Our primary interest is the possible improvements resulting from including EKA in our automatic monitoring of North Sea seismicity, and for the 10-month period we have compared the results of the two GBF processes (with or without EKA) for the general North Sea region (53°N-65°N, 5°W-10°E). Table 6.1.1 shows a subset of the processing results comprising those events in this region that fulfil the following criteria:

- At least two arrays with both a P-type and an S-type detection
- At least one P-type detection at the EKA array

These criteria are generally sufficient to ensure that the event is real, and the condition of at least one detected EKA P-phase would imply that the reliability of the event location would be improved because of the improved azimuthal coverage. We have reviewed all of the 40 events listed in Table 6.1.1, and found only two events (marked by X in the rightmost column) that are considered to be of questionable quality.

Table 6.1.1 List of selected seismic events in the North Sea general region during December 2013 through September 2014. The list comprise all events that fulfil the detection requirements specified in the text. The distance (km) from EKA and NORES (NRS) as well as the signal-to-noise ratio (SNR) at these two arrays are indicated for each event. Those events that have been included in the NORSAR reviewed regional bulletin are marked with N in the right hand column, whereas two events that have been determined to have a mis-associated phase and therefore are not considered acceptable are marked by X in that column.

	Origin time	Lat	Lon	Mag	Region	EKAdist	EKASNR	NRSdist	NRSSNR	
1	2013-335:08.13.58.0	57.05	7.06	2.02	EASTERN NORTH SEA	662.00	44.00	485.70	59.20	-
2	2013-335:09.48.17.0	60.63	1.80	2.88	VIKING GRABEN	659.00	348.50	532.40	1264.00	N
3	2013-339:14.26.47.0	58.44	6.10	1.61	ROGALAND NORWAY	661.80	4.80	399.70	41.60	-
4	2013-344:14.19.49.0	58.44	6.48	1.74	ROGALAND NORWAY	681.80	5.10	383.20	76.80	N
5	2013-344:21.07.17.0	56.90	7.84	2.68	EASTERN NORTH SEA	705.30	60.20	478.30	160.40	N
6	2013-354:14.18.26.0	58.64	5.90	1.68	ROGALAND NORWAY	662.30	4.00	394.20	33.70	N
7	2014-006:14.16.40.0	58.24	6.30	1.41	ROGALAND NORWAY	662.20	4.10	406.70	11.70	-
8	2014-014:14.19.12.0	58.24	6.68	1.15	AGDER NORWAY	682.60	3.50	391.20	10.60	-
9	2014-016:17.09.34.0	59.19	1.77	2.42	VIKING GRABEN	522.80	34.70	572.10	39.50	N
10	2014-021:06.39.03.0	61.02	5.09	2.46	SOGN-MOERE REGION NORWAY	797.00	3.50	351.90	145.40	N
11	2014-023:04.32.50.0	61.22	4.90	2.70	NORTHERN NORTH SEA	807.60	9.30	363.90	446.20	N
12	2014-030:14.20.28.0	58.44	6.10	1.38	ROGALAND NORWAY	661.80	3.60	399.70	21.60	-
13	2014-043:14.22.54.0	58.05	6.87	1.92	SKAGERRAK	684.20	3.50	400.50	14.50	-
14	2014-044:02.13.16.0	53.68	6.56	2.54	NORTHERN LOWER SAXONY AND HOLSTEIN	655.90	53.10	841.50	145.10	-
15	2014-060:13.58.05.0	57.02	7.34	2.64	EASTERN NORTH SEA	678.20	49.10	479.60	115.00	-
16	2014-072:14.20.30.0	58.24	6.30	1.22	ROGALAND NORWAY	662.20	5.80	406.70	28.90	-
17	2014-084:11.55.26.0	60.98	6.25	1.29	SOGN-MOERE REGION NORWAY	837.10	3.30	289.10	25.30	-
18	2014-084:18.19.55.0	57.09	7.28	1.65	EASTERN NORTH SEA	676.20	6.30	474.60	13.90	-
19	2014-092:17.46.32.0	58.64	5.90	1.64	ROGALAND NORWAY	662.30	4.60	394.20	31.80	-
20	2014-098:06.50.13.0	62.27	3.76	2.79	MOERE SHELF	869.50	8.70	448.60	50.50	-
21	2014-120:13.19.24.0	58.44	6.10	1.26	ROGALAND NORWAY	661.80	4.10	399.70	15.70	-
22	2014-122:14.06.55.0	61.39	7.39	0.58	SOGN-MOERE REGION NORWAY	913.40	4.30	235.80	14.70	X
23	2014-122:18.13.00.0	53.40	2.67	2.96	SOUTHWESTERN NORTH SEA	435.40	359.20	976.90	8.20	N
24	2014-125:13.34.36.0	62.34	4.05	2.51	MOERE SHELF	884.00	4.40	436.50	35.40	N
25	2014-128:13.20.31.0	58.05	6.87	1.49	SKAGERRAK	684.20	4.80	400.50	25.90	-
26	2014-143:13.18.51.0	58.44	6.48	1.90	ROGALAND NORWAY	681.80	4.10	383.20	27.50	N
27	2014-154:13.17.25.0	58.24	6.68	1.36	AGDER NORWAY	682.60	4.90	391.20	19.00	-
28	2014-160:18.01.26.0	64.01	6.35	1.80	VOERING BASIN	1103.30	3.90	453.00	28.30	N
29	2014-161:13.19.48.0	58.24	6.30	1.42	ROGALAND NORWAY	662.20	4.30	406.70	18.10	-
30	2014-199:13.23.18.0	58.24	6.30	1.78	ROGALAND NORWAY	662.20	9.60	406.70	42.40	-
31	2014-218:12.33.37.0	53.59	-1.82	2.17	PENNINES	212.80	14.70	1131.40	4.80	X
32	2014-228:01.18.42.0	57.02	6.97	1.38	EASTERN NORTH SEA	656.40	13.90	490.40	14.70	-
33	2014-241:09.24.56.0	55.49	7.88	1.44	EASTERN NORTH SEA	699.00	9.30	622.50	11.90	-
34	2014-241:13.19.10.0	58.24	6.68	1.90	AGDER NORWAY	682.60	6.30	391.20	27.00	N
35	2014-249:16.56.37.0	60.15	6.03	2.50	HARDANGER NORWAY	765.90	5.60	310.40	218.60	N
36	2014-250:05.01.56.0	58.02	6.80	1.96	SKAGERRAK	679.80	4.70	404.70	21.40	N
37	2014-252:13.14.52.0	58.24	6.68	1.41	AGDER NORWAY	682.60	3.50	391.20	23.50	-
38	2014-266:13.19.38.0	58.44	6.10	1.28	ROGALAND NORWAY	661.80	4.00	399.70	26.00	-
39	2014-273:10.59.04.0	58.65	0.47	2.89	VIKING GRABEN	430.10	44.80	665.10	51.00	N
40	2014-275:13.18.49.0	58.44	6.10	1.69	ROGALAND NORWAY	661.80	5.40	399.70	20.40	-

We note that most of the events listed in Table 6.1.1 have not been included in the NORSAR reviewed regional bulletin. This is mainly because the event magnitude is below the threshold for such analysis. However, more importantly, such events can now be extracted and presented to the analyst without generating a large number of false alarms which would previously have been the case (this is because of the restrictive criteria that are now applied to generate Table 6.1.1). The two 'false alarms' in Table 6.1.1 are easily removed by the analyst; they might in fact be real events, but would be of no interest to monitoring the North Sea area.

A map showing the location of the 38 acceptable seismic events in Table 6.1.1 is shown in Figure 6.1.7. We note from this figure that the geographical distribution of the detected events is as expected, considering the overall seismicity pattern shown in Figure 6.1.2. The main seismicity is near the Norwegian west coast. As a consequence, the epicentral distances of the detected events are generally larger for EKA than for NRS, and the signal-to-noise ratio at NRS is in most cases somewhat higher than at EKA. Figure 6.1.8 shows SNR at the two arrays adjusted for event magnitude as a function of distance, and confirms a slightly better detectability for NRS for this event set. Nevertheless, we can conclude that EKA has an excellent performance for event detectability in the North Sea region, and would provide a very valuable supplement to the NORSAR regional GBF processing.

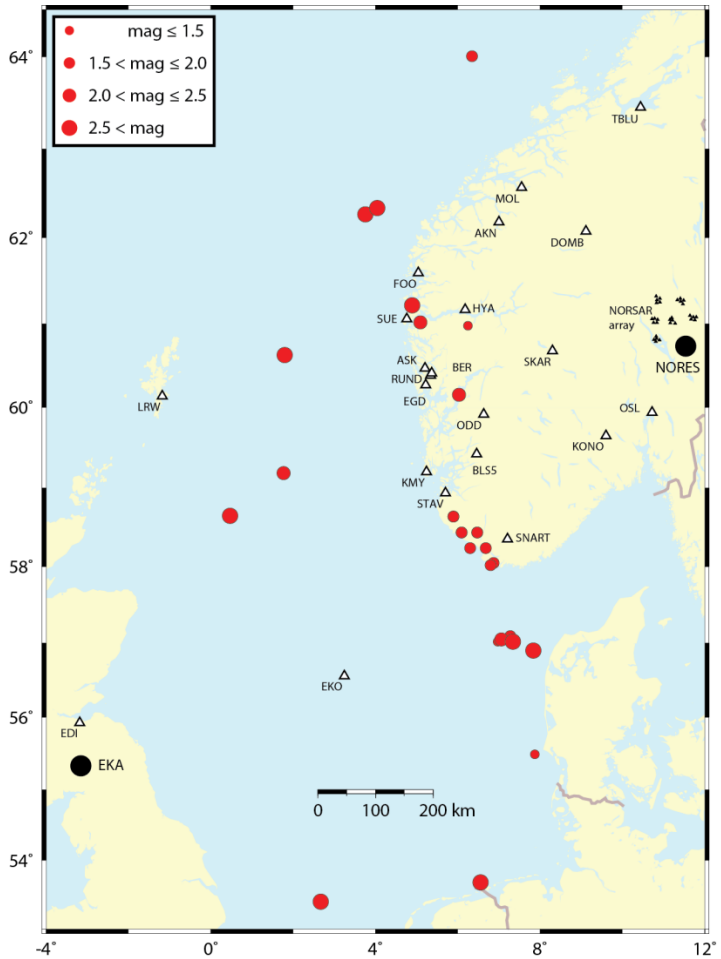

Fig. 6.1.7 Automatic location of the 38 acceptable seismic events listed in Table 6.1.1. Note that because the GBF procedure is grid-based, some events nearby each other will be located at the same grid point in the automated GBF procedure.

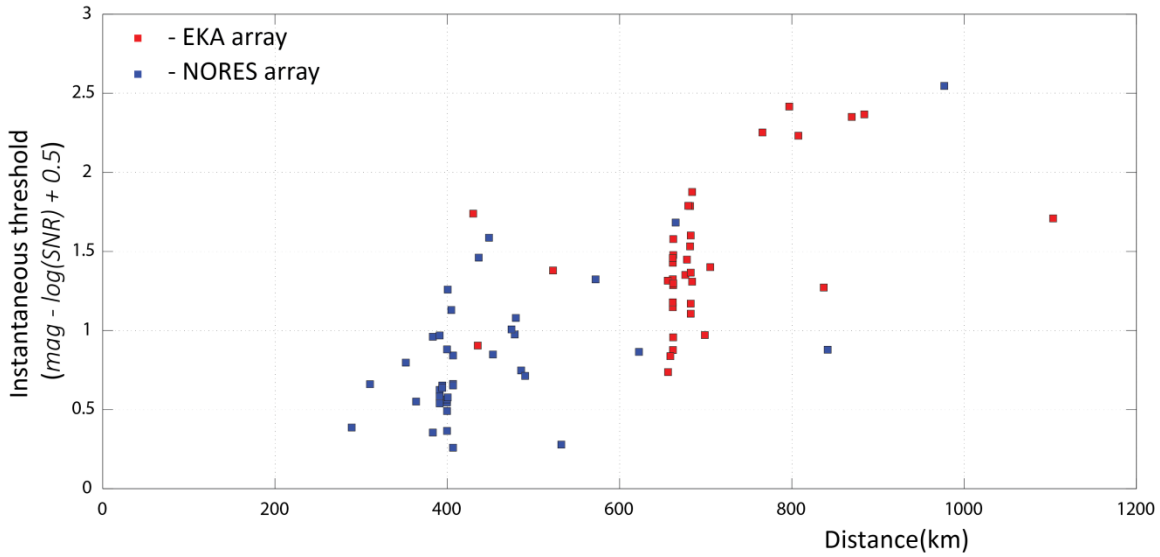

Fig. 6.1.8. SNR at the two arrays adjusted for event magnitude as a function of distance,

6.1.4 Conclusions

Our conclusions from this study are as follows:

- The EKA functions as an excellent regional array, and could be a very valuable supplement to NORSAR's regional seismic network.
- Inclusion of EKA in the NORSAR GBF processing works very well. EKA detections have been automatically associated with many seismic events already detected by the regular GBF processing during the time period.
- With EKA included, the NORSAR GBF detection list contains many small events in the North Sea region currently not being analyzed interactively at NORSAR. Thus, the inclusion of EKA would contribute to a more complete reviewed NORSAR regional bulletin.
- In addition, the inclusion of EKA results in many new seismic events being detected. However, most of the new events are one-array events (P and S from EKA) in or close to Britain, and are therefore not candidates for inclusion in the NORSAR regional bulletin.
- Addition of EKA gives a much improved azimuthal coverage for detected events, thus providing more accurate event locations.
- The array beams formed with EKA data give significant SNR improvements, thus enabling more precise phase arrival time estimates.

There are still some remaining improvements that could be considered. Thus, the EKA array data is currently processed using a generic recipe. Improved performance can be achieved by conducting a tuning study. The automatically calculated magnitudes at EKA have not yet been calibrated, and this obviously needs to be done. There might also be a need for considering Lg blockage across the Viking Graben (Kennett et al., 1985) when forming the generalized beams. Such blocking features occur also in other areas covered by the NORSAR regional processing, and should be considered there as well.

F. Ringdal
T. Kværna
J. Schweitzer

References

Kennett, B.L.N., S. Gregersen, S. Mykkeltveit and R. Newmark (1985). Mapping of crustal heterogeneity in the North Sea basin via the propagation of L_g-waves. Geophys. J. R. astr. Soc. **83**, pp. 299-306.

Kværna, T., J. Schweitzer, L. Taylor and F. Ringdal (1999). Monitoring of the European Arctic using Regional Generalized Beamforming. In: NORSAR Sci. Rep. 2-98/99, Kjeller, Norway, 78-94.

Ringdal, F. and T. Kværna (1989). A multi-channel processing approach to real time network detection, phase association, and threshold monitoring. Bull. Seism. Soc. Am. **79**, No. 6, pp. 1927-1940.

Ringdal, F. and T. Kværna (2004): Some aspects of regional array processing at NORSAR. In: NORSAR Sci. Rep. 1-2004, Kjeller, Norway, 34-44.

Schweitzer, J and T. Kværna. (2006). Improvements to SPITS regional S-phase detection: coherent beamforming of rotated horizontal components In: NORSAR Sci. Rep. No. 2-2006, Kjeller, Norway, 47-58.

6.2 The modernized large-aperture broadband array NOA

6.2.1 Introduction

The NORSAR seismic array NOA has been operational since 1970. Originally it consisted of 22 sub-arrays with 132 borehole sites and 22 vault sites distributed over an area with approximately 120 km diameter. The borehole sites were equipped with HS-10 vertical short-period seismometers and the vault sites with Teledyne Geotech 8700 three-component long-period sensors, and data were recorded with Philco-Ford 8 bit gain-ranged digitizers. In 1976 the size of the array was reduced to 7 subarrays (42 HS-10 and 7 Teledyne-Geotech 8700) and in 1994 the Philco-Ford digitizers were replaced by Nanometrics RD6 digitizers. A major refurbishment was conducted in 1994-1995 by installing new sensors (42 Teledyne Geotech 20171 short-period and 7 Teledyne Geotech KS54000 borehole broadband sensors) and digitizers (Science Horizons AIM24) at all sites. In year 2000 one of the KS54000 was replaced by a Güralp CMG-3T in order to comply with the CTBTO requirements for certification as IMS station, but otherwise the configuration was unchanged until 2011.

The planning for the latest modernization/recapitalization of the NORSAR array in 2011 started already in 2006. The equipment became obsolete/outdated and was not supported anymore by the manufacturer. The proper operation of the array was at risk due to the lack of spare parts. It took about 2 – 3 years to obtain the necessary funding for the refurbishment of the complete NOA array (jointly financed by CTBTO and Norwegian Ministry of Foreign Affairs). Equipment specification, procurement, prototype testing and several rounds of prototype revisions required another 2 years. The installation of the new equipment was distributed over half a year, with one subarray completed at any time, so that the IDC could retain station NOA in operations with reduced configuration, while testing the new configuration in a testbed. On July 5, 2012, the last site of the NOA array had been upgraded.

The continuous operation of the NORSAR array through more than 40 years provides a unique archive of historic seismological data of nuclear explosions, earthquakes, natural and man-made events. For the years 1971-1983, events were selected for archiving, but after 1983 all continuous data are archived. All available data for the complete time period are online, easy accessible on disk and open to the public.

6.2.2 Location and infrastructure

The NOA array has a diameter of about 60 km and its 42 sites are arranged in 7 sub-arrays (NAO, NBO, NB2, NC2, NC3, NC4, NC6) with sub-array diameters of 6 – 8 km and 6 sites each (Figure 6.2.1). Each sub-array has 5 borehole sites (BH), one vault site (VS) and a central terminal vault (CTV) with power and communication (the vault sites and the borehole sites where earlier called long-period vaults and short-period sites, respectively, but this is somewhat misleading now, because after the upgrade all sites are equipped with broadband instruments). The power system in the CTVs receives power from the public grid and charges a UPS with a battery bank providing about 3 days operation capacity for the entire sub-array. Each site of the sub-array is individually connected by a single cable with the CTV. These cables (some of them as long as 14 km) provide DC-power as well as communication to the sites. In total the array has about 155 km of cable trenches, affecting 127 landowners.

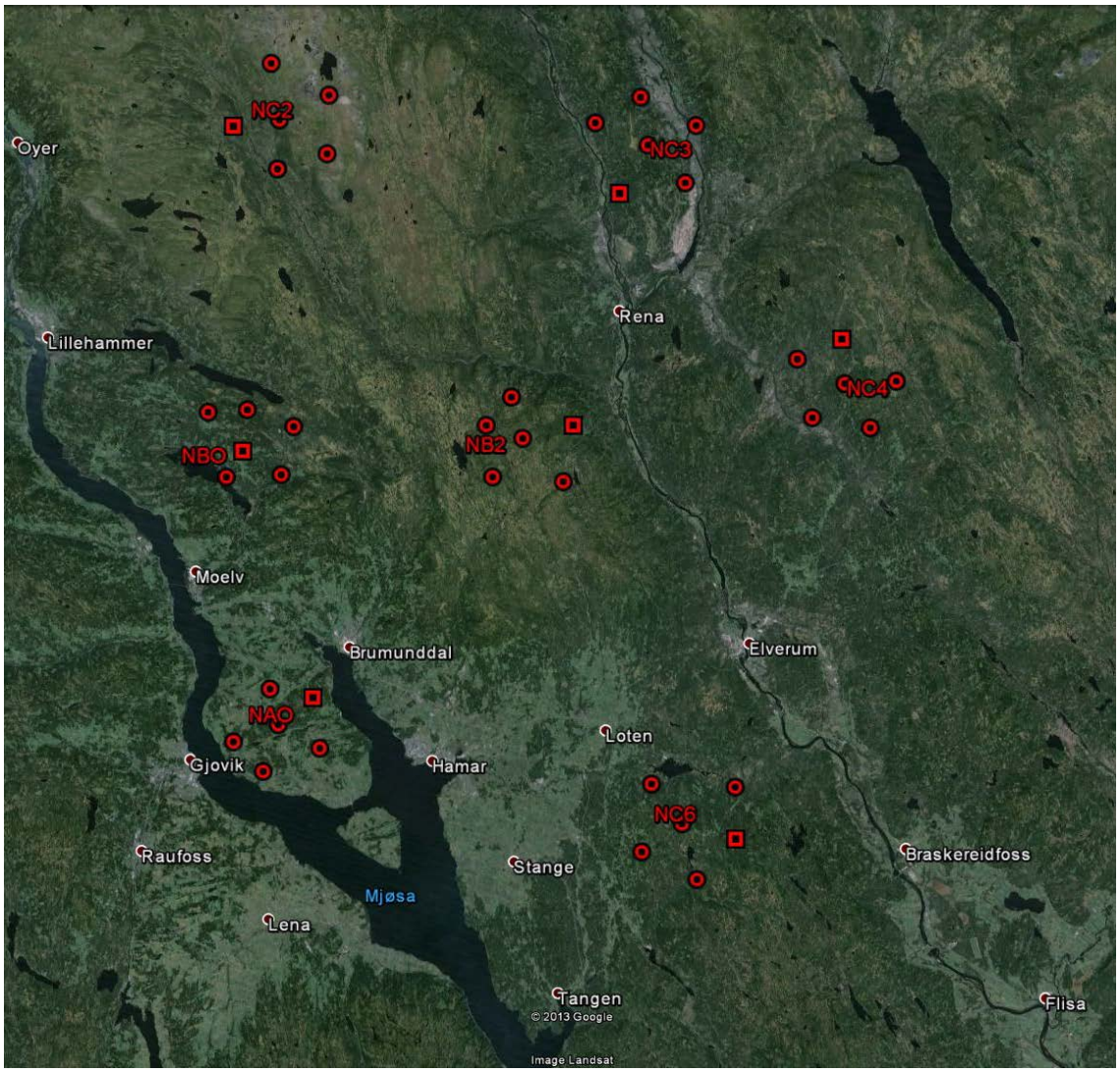

Fig. 6.2.1. Map of the NOA array. Borehole sites are marked with circles, vault sites with adjacent terminal vaults are marked by squares. The yellow line indicates a 20km scale.

Representative for all CTVs, Figure 6.2.2 shows the Central Terminal Vault at sub-array NAO. The picture was taken in 2012 during the migration to a new VSAT technology and the repointing of the satellite dishes. Originally the CTVs did not have the small superstructure, which was cumbersome in wintertime since then the door of the actual vault opened upwards and the snow height can easily reach 2 meters. The picture on the right hand side shows the equipment inside of the CTV, i.e., the rack with modems and lightning protection cards, the power distribution box, the UPS and the battery rack. From the CTV, 48 V DC is distributed to the 6 sites. The communication is established by modems and PPP-protocol. Due to the long-distance cables our transmission rate is limited to 38400 bit/s (19200 bit/s for the most remote site).

Figure 6.2.3 shows the entrance and the interior of the vault site at NC6. Only one of the three pits is used for the regular operation the remaining pits are free for instrument testing. An example of a borehole site is given in Figure 6.2.4. Under normal conditions only the GPS mast and the lid of the site is visible. The digitizer and the pit boxes are installed in a drum on top of the borehole. The sensor is down on the bottom of the borehole securely locked to the borehole wall with a clamping mechanism.

Fig. 6.2.2. Central Terminal Vault (CVT) at NAO. In 2012 NORSAR migrated to new VSAT technology and the antenna dish needed to be pointed to a new satellite. Right: Inside of the CVT. From left to right: rack with modems and power distribution to pits, cable box to pits with coarse lightning protection, and uninterruptable power system with battery rack.

Fig. 6.2.3. Vault site (VS) at NC6. The VSs have 3 pits (formerly used for the 3 components of long-period sensors). With the current installation only one of the pits is used.

Fig. 6.2.4. Borehole site (BS) NC601. The sensor is installed in a shallow (down to 12 m depth) borehole. A zinc drum on top of the borehole contains the digitizer (Güralp CMG-DM24S3EAM), a power and communication pit box (lightning protection, battery power charger, Patton modem, 12V 800mAh battery bank) and a junction box (coarse lightning protection and 48/12 DC/DC converter).

6.2.3 Instrumentation

The recapitalization of the NOA array comprised new acquisition computers for the 7 CTVs, modified pit boxes, new digitizers and new sensors; the communication/power cables, UPSs, vaults and boreholes were not included in this upgrade (but are maintained on a regular basis).

All sites are equipped with Güralp CMG_DM24S3AM acquisition modules. These allow for remote control of the sensors (lock, unlock, center, calibrate, etc.), state-of-health and tamper monitoring, local data storage (set up for a 14-days buffer), data signing and realtime data transmission to the CTV.

The decision to install Güralp seismometers, with a hybrid instrument response, was made after careful analysis of the noise conditions on all our arrays (NOA, ARCES and SPITS), the experiences with the existing systems and the need to have a good monitoring capability for both regional high-frequency/low-magnitude events as well as global low-frequency/high-magnitude earthquakes. Furthermore, the intention was to use this type of instrument also for the later recapitalization of the ARCES array. The hybrid response function was specified by NORSAR and engineered by Güralp. This process involved comprehensive testing of the instruments (but also of the digitizers) and adjustments (e.g., Roth et al. 2011). Table 6.2.1 contains the system responses of the two new sensor types: (i) for the 3-component very-broadband sensor (CMG-3T Hybrid 360s – 50Hz) in a surface-mount casing and (ii) for the vertical-component broadband sensor (CMG-3V 120s – 50 Hz) in a

borehole casing. The seven vault sites of NOA have been equipped with the 3-component sensor and the 35 borehole sites have been equipped with the vertical-component sensor. The transfer functions for both models are identical for frequencies above 0.2 Hz (see Figure 6.2.6), which allows array processing of all data for that frequency range without instrument correction. For frequencies above 0.01 Hz the amplitude response is identical and only the phase response differs. However, array processing tests with long period data show that these phase response differences can be neglected for frequencies above 0.02 Hz.

CMG-3T Hybrid 360s - 50Hz		CMG 3V Hybrid 120s – 50 Hz	
2x20000 V/m/s @ 5Hz		2x20000 V/m/s @ 5Hz	
3 Zeroes	7 Poles	3 Zeroes	7 Poles
0	-2	0	-2
0	-1.964E-3±1.964E-3j	0	-5.89E-3+5.89E-3j
-0.3333	-24±21j	-0.3333	-24±21j
	-41±114j		-41±114j

Table 6.2.1. Poles and zeroes (in units of Hz) defining the velocity response of the hybrid sensors.

Figure 6.2.5 shows instrument responses for a variety of NORSAR installations (for a complete overview see Pirli, 2013). Two short-period systems (the Teledyne instruments formerly installed in the NOA borehole sites and the GS13 sensors of the NORES array), two broad-band systems proportional to acceleration (the KS54000 formerly installed in the NOA vault sites and Güralp 3T of the SPITS array), four broad-band systems proportional to velocity and the two new broad-band systems with hybrid response (bold, dashed lines). The absolute levels of the hybrid systems match the levels of the short-period systems, the SPITS and NOA broadband systems for a frequency of about 5 Hz.

Figure 6.2.6 compares the former NOA instrumentation with the new one. The plots show the velocity responses in order to highlight the 2 different plateaus of the hybrid response. The new systems are proportional to velocity for frequencies from 0.01Hz (0.005Hz) to about 0.2Hz and for frequencies between 3 – 20Hz. In the intermediate range, the instruments are proportional to acceleration. Traditionally, sensors are either proportional to ground velocity or to ground acceleration. The new sensor type is both and therefore its name ‘hybrid’. The advantage of the hybrid sensor is its ability to record weak regional/local high-frequency events with sufficient gain as well as strong earthquakes in regional/global distances. A velocity-proportional sensor adjusted for weak high-frequency events would clip for signals of large magnitude earthquakes in regional/global distances (as observed for instance for our broad-band sensor at ARCES (see Figure 6.2.5). On the other hand, a velocity-proportional sensor adjusted for the monitoring of regional/global earthquakes, would not have enough gain to properly monitor high-frequency explosions at regional distances, which are of interest.

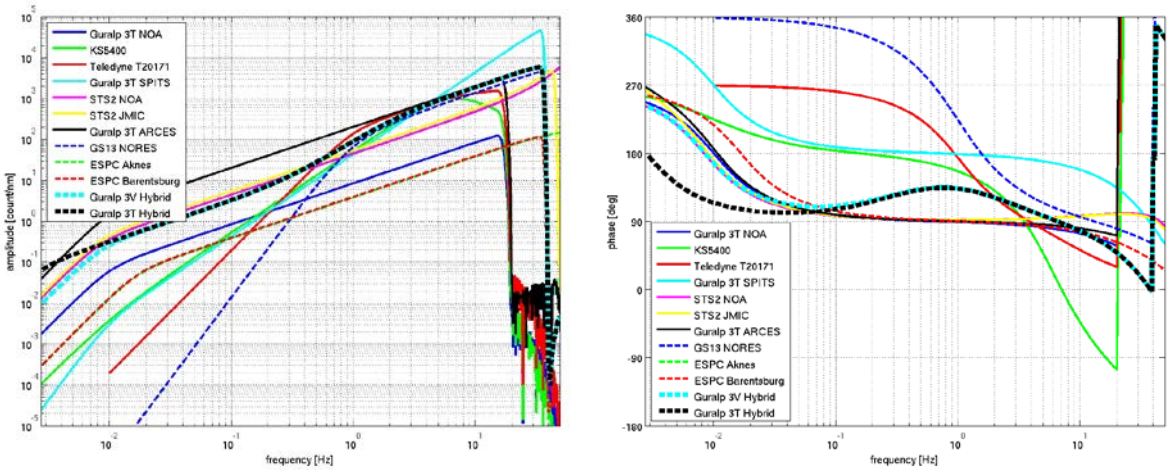

Fig. 6.2.5. System responses of various NORSAR installations. Left: Displacement amplitude response, right: phase response.

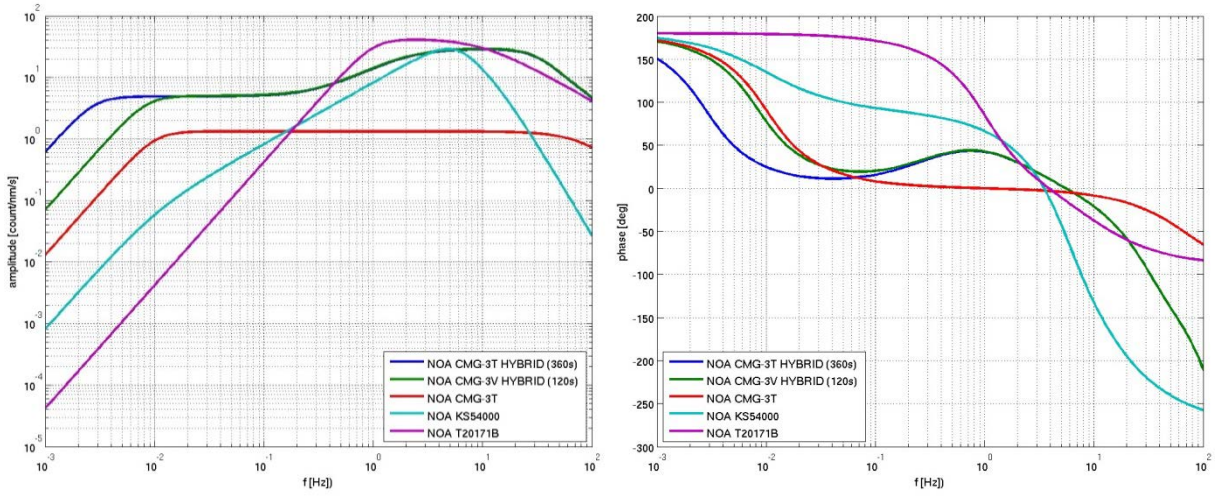

Fig. 6.2.6. System responses of the old (CMG-3T, KS54000, T20171B) and new NOA instrumentation (CMG 3T Hybrid (360s), CMG 3V Hybrid (120s)). Left: Velocity instrument responses, right: phase responses.

Figure 6.2.7 (left) shows the setup for coherency tests for the CMG 3V borehole sensors in the basement of our field laboratory in Hamar. Two prototype instruments had been tested thoroughly for a longer time period in our facility at Stendammen. This was not possible for the major bulk of the instruments, but all of them were checked with respect to instrument noise, mass drift, temperature dependency, waveform coherency, etc. for at least several days at our field lab. The picture on the right hand side of Figure 6.2.7 shows a borehole sensor with mounted hole lock just before deployment. The sensors are lowered to the bottom of the boreholes (8 – 12m deep) and locked to ensure good coupling. In addition, a rubber foam plug was installed in the borehole close to the top of the instrument. The plug minimizes the air volume around the sensor and therefore decreases noise due to thermal convection. Figure 6.2.8 shows an opened Güralp 3T Hybrid sensor and on the right hand side the pit where it was eventually installed. Like for the borehole installations a good thermal insulation helps to avoid long-period noise due to air convection around the sensor.

Fig. 6.2.7. Güralp CMG-3V Hybrid borehole sensors. Left: Test setup, right: just before installation with hole lock attached.

Fig. 6.2.8. Güralp CMG-3T HYBRID sensor. Left: Cover removed, right: installed in one of the vault pits. The sensor is covered with an insulation tube.

The deployment of the sensors and digitizers was done in several stages. In June 2011, the 3-component instruments were deployed (CMG-3T HYBRID) into the 7 vault sites and the obsolete equipment (6 KS54000 sensors, 1 CMG-3T standard, 7 Nanometrics digitizers) were removed. The original 42 short-period instruments remained in place (35 borehole sites and 7 vault sites) for the time being, because the CMG-3V borehole instruments were still in a test phase mainly with issues of mass drift. In September 2011, the decision was made NOT to start with the upgrade of all sites that late in autumn. Early snowfalls could have prevented the completion and then the NOA array would have been difficult to operate during the winter with the mixed instrumentation. However, in October 2011, one of the short-period borehole instruments in each subarray was replaced with a new CMG-3V. This decreased the overall performance of the NOA array (to an acceptable degree), but performance and reliability of the new equipment could be tested in winter conditions. Finally, during the time period April – June 2012, the upgrade of the remaining NOA sites was completed (see Table 6.2.2 for the startup of the sites). The modernized NOA array has been operational since summer 2012.

Site	start	Site	start	Site	start	Site	start
NAO00	15.05.2012	NBO00	**20.06.2011**	NB200	20.06.2012	NC200	21.06.2012
NAO01	**20.06.2011**	NBO01	15.08.2012*	**NB201**	**20.06.2011**	NC201	27.04.2012.
NAO02	14.05.2012	NBO02	25.08.2012*	NB202	16.06.2012	NC202	14.06.2012
NAO03	**25.10.2011**	NBO03	**25.10.2011**	NB203	20.06.2012	**NC203**	**21.10.2011**
NAO04	15.05.2012	NBO04	24.05.2012	**NB204**	**19.10.2011**	**NC204**	**20.06.2011**
NAO05	15.05.2012	NBO05	15.08.2012*	NB205	20.06.2012	NC205	05.07.2012
NC300	14.06.2012	NC400	07.06.2012	NC600	23.05.2012	*) sites were installed but power/communication cables had been damaged during road construction and could not be repaired before August 2012	
NC301	**14.10.2011**	NC401	14.06.2012	NC601	25.05.2012		
NC302	07.06.2012	NC402	07.06.2012	**NC602**	**20.06.2011**		
NC303	**20.06.2011**	**NC403**	**20.10.2011**	NC603	23.05.2012		
NC304	15.06.2012	NC404	14.06.2012	NC604	23.05.2012		
NC305	07.06.2012	**NC405**	**20.06.2011**	**NC605**	**25.07.2011**		

Table 6.2.2 Startup times of new hybrid sensors at NOA sites (upgrades in 2011 are marked in bold face). The last site was installed 5th July 2012,

Figure 6.2.9 compares the old and new distribution of broadband sensors in the NOA array. Going from 7 to 42 broadband sensors improves the array transfer function especially for long-period signals, e.g., surface waves and provides high channel redundancy.

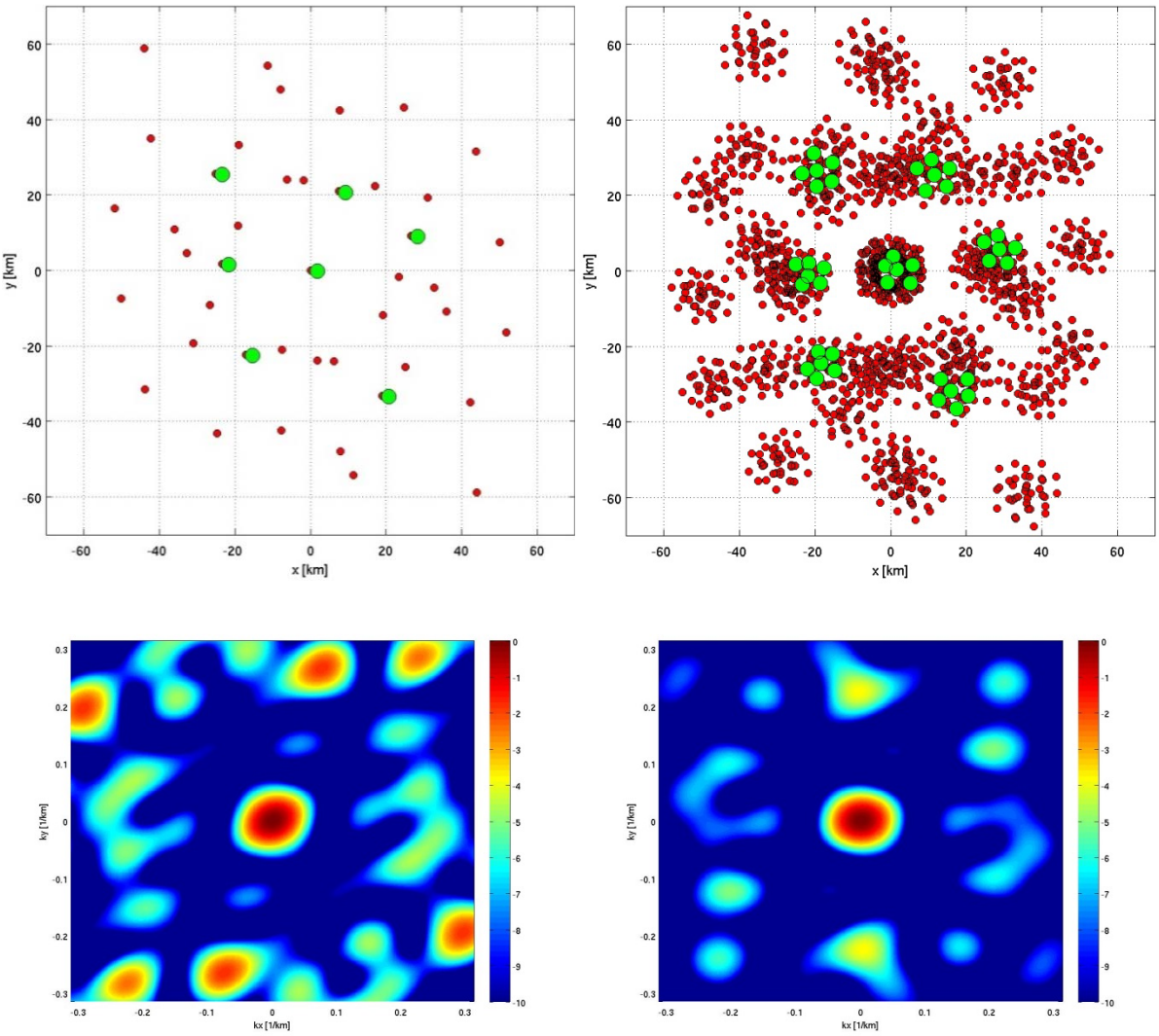

Fig. 6.2.9. Top: Array sites (green dots) and co-array (red dots) for NOA broadband sites. Left: old configuration with 7 broadband sites, Right: new with 42 broadband sites. Bottom: Broadband array response. Left: with the original 7 broadband sites. Right: with the 42 broadband sites.

6.2.4 Data and processing examples

6.2.4.1 Comparison of old and new sensors

After installation of the new hybrid instruments, several tests were performed to compare old and new data-processing results. During a transition period in autumn 2011, the KS54000 and the new NORSAR 360 s CMG-3T Hybrid instruments were co-located and recorded in parallel. Figure 6.2.10 shows beams of the vertical components (KS54000: BEAM-1, CMG-3T Hybrid: BEAM-2) for a surface wave in the long-period frequency range (15–30 s) from a M_S 4.4 earthquake in Turkey (29.10.2011, 22:24:22.9, 38.82N, 43.43E, depth: 0 km, distance: ~ 3250 km). The data for the seventh 3C site (NC602) were simulated from the old CMG-3T broadband sensor. The signal-to-noise ratio (SNR) is improved by a factor of about 1.6 for the new instrumentation.

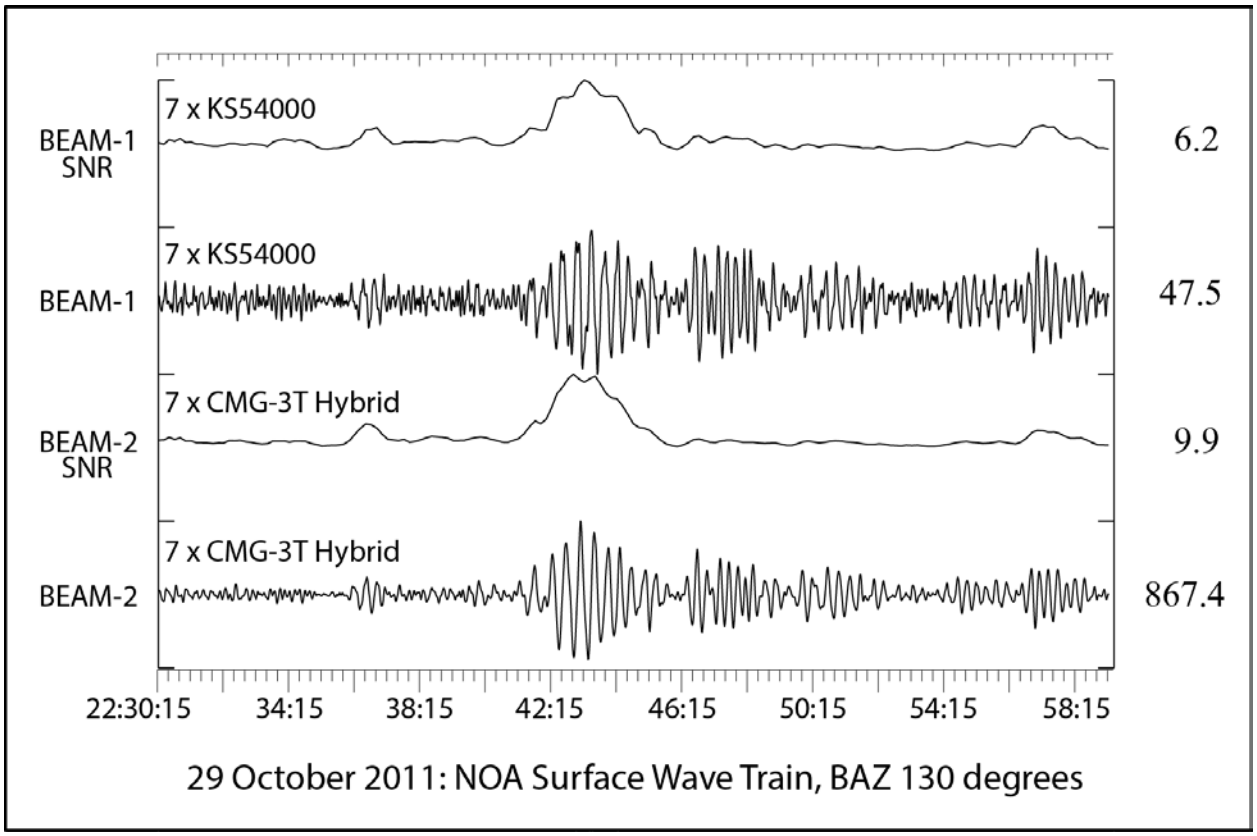

Fig. 6.2.10 Shown are the surface-wave beams calculated from the seven 3C instruments of NOA using the old (BEAM-1) and the new (BEAM-2) sensors and the corresponding SNR traces. The data were Butterworth bandpass filtered between 10 and 20s.

The frequency-wavenumber (fk) results for the seven vertical components of the same data are shown in Figure 6.2.11 (on the right: KS54000, on the left: CMG-3T Hybrid) and are very similar. However, comparing the size and amplitude of the two side lobes it is clear that they are a bit smaller and less pronounced for the new instrumentation. This improvement is due to the larger bandwidth of the new instrumentation.

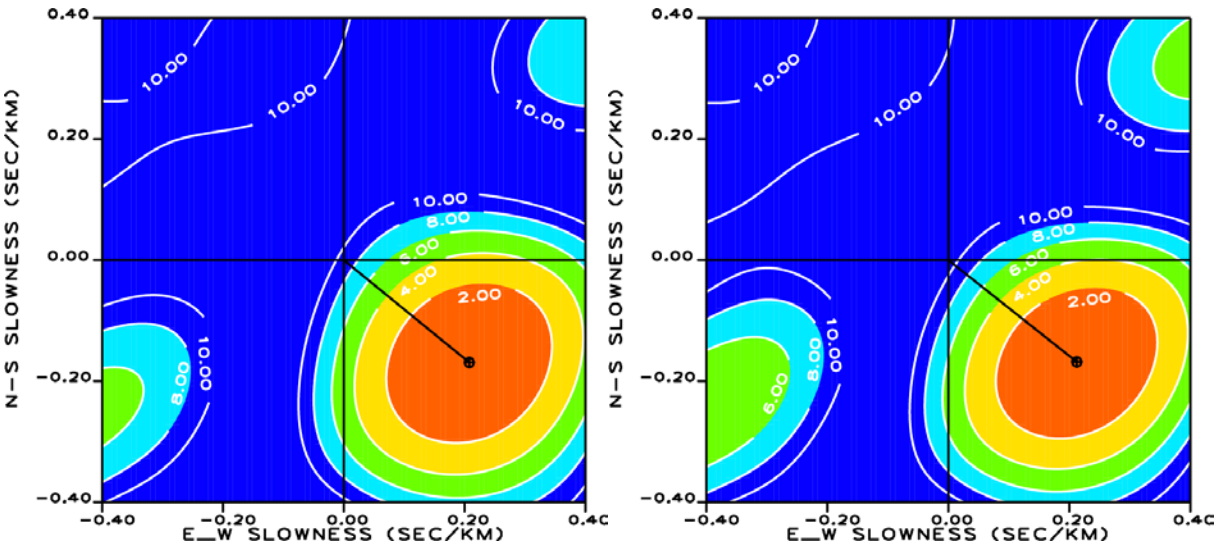

Fig. 6.2.11. Fk results for surface-wave trains of the 29 October 2011 event in Turkey, used were the seven vertical traces of the 3C sensors: the result for the seven KS54000 instruments are shown on the left and result for the seven new CMG-3T Hybrid sensors on the right.

6.2.5 Comparison of array configurations

After the whole array had been equipped with new CMG-3T Hybrid sensors, the array recorded surface waves generated by the 15 February 2013 Chelyabinsk Meteor impact (~3000 km distance). The LR phase is clearly visible on the records of all sites after bandpass filtering between 20 and 50 s (or 0.02 and 0.05 Hz). These data were used for the following study. Figure 6.2.12 shows as top trace (labelled NAO01s) an example for a single station recording the data of site NAO01 after simulating a KS54000 instrument. The third trace from top (labeled NAO01) shows the original CMG-3T Hybrid record. Although identically filtered these two traces already show the principle difference between the new and the old instrumentation: the new instrumentation has a higher sensitivity and the low frequency contents is larger. The other traces show beams calculated for different configurations. For BEAM-1 only the KS54000 simulated vertical traces of the 3C sites were used to simulate the old NOA surface wave capability, for BEAM-2, the unchanged CMG-3T Hybrid vertical traces of the 3C sites were used to show the improvement by the new instrumentation and finally for BEAM-3, the 40 available CMG-3T Hybrid vertical traces were used (two sites out of the 42 were down) to demonstrate the new NOA capabilities to observe and analyze seismic surface waves. The SNR improvement with the new instruments is significant as well as the larger dynamic range.

The fk-results for the three array configurations are shown in Figure 6.2.13. The results for the two 7 element arrays (for BEAM-1 on the left and for BEAM-2 in the middle) differ not much. This is in agreement with the above shown example (Figure 6.2.11). But the side-lobe suppression for the fk-analysis is significantly improved, when using the 40 available broadband elements of the new NORSAR array (for BEAM-3, on the right).

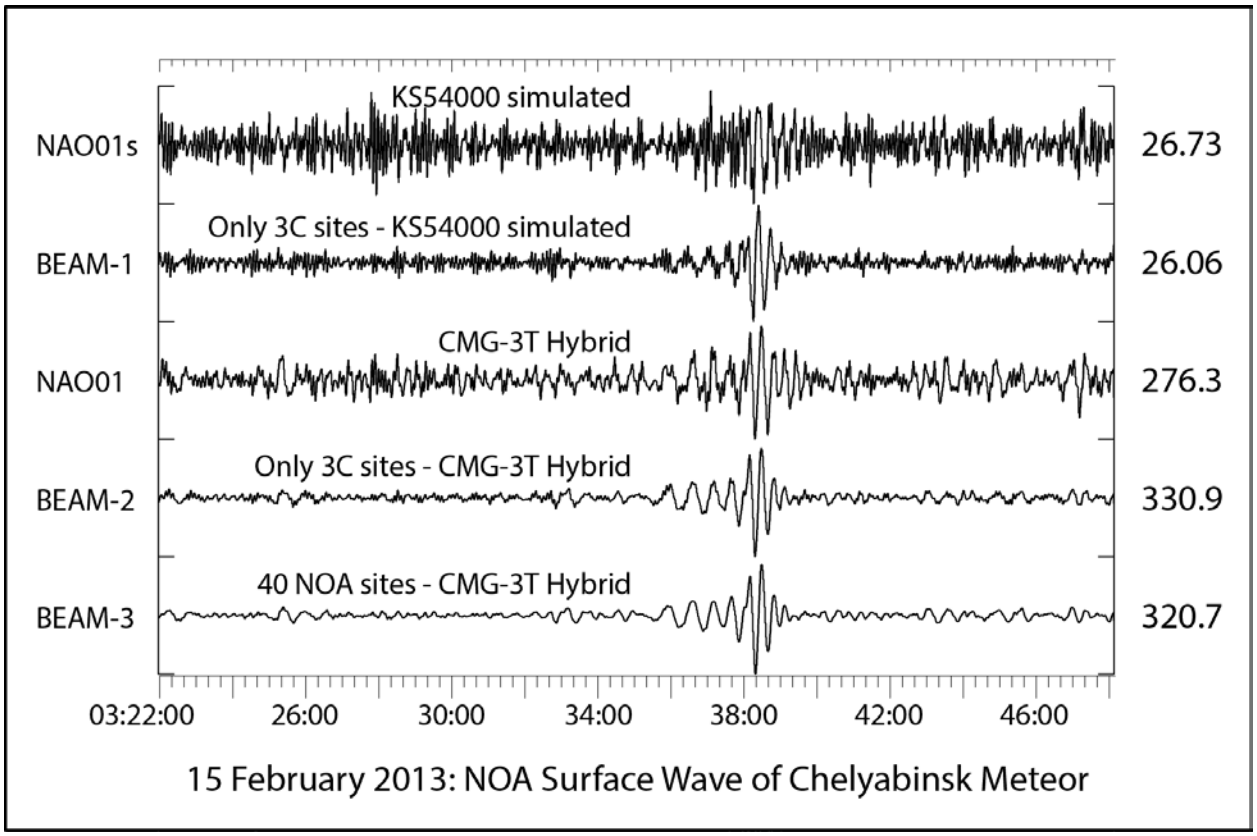

Fig. 6.2.12. The figure shows bandpass filtered (20 – 50 s) surface wave observations generated by the Chelyabinsk Meteor impact (~3000 km distance). The top trace (NAO01s) shows a KS54000 simulation for the recording at NOA site NAO01, the second trace (BEAM-1) shows a beam of the simulated KS54000 recordings from all the 7 sites with 3C instrumentation, corresponding to the old NORSAR array configuration. The middle trace (NAO01) shows the CMG-3T Hybrid recording at NORSAR array site NAO01. The lower two traces show array beams of the new NORSAR Hybrid instrumentation data; BEAM-2 for the 7 sites with 3C instrumentation and BEAM-3 for all 40 available NORSAR array elements.

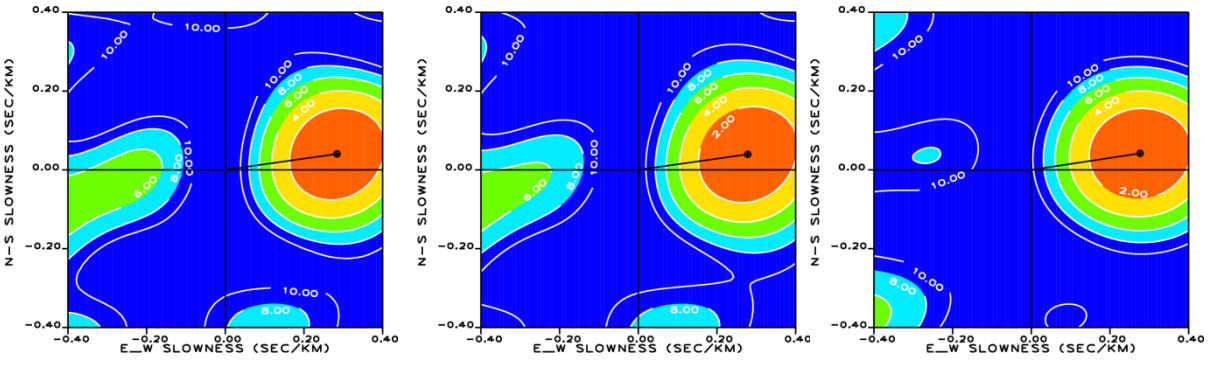

Fig. 6.2.13. Shown are the fk-analysis results for the three beam configurations of Figure 6.2.12. The results for the two 7 element arrays for BEAM-1 on the left and for BEAM-2 in the middle. The fk-analysis result for the 40 available broadband elements of the new NORSAR array (BEAM-3) is shown on the right.

6.2.6 Time corrections for the new NOA broadband array

Figure 6.2.14 shows, the vertical component recordings at the NOA site NB200 from two events in Iran (left: 16 April 2013, Mw 7.8; right: 12 May 2013, M 5.6), unfiltered (at the top) and filtered with different bandpass filters. It is obvious that the dominant frequency range varies for the different seismic phases. However, the smaller event cannot be observed at all frequencies.

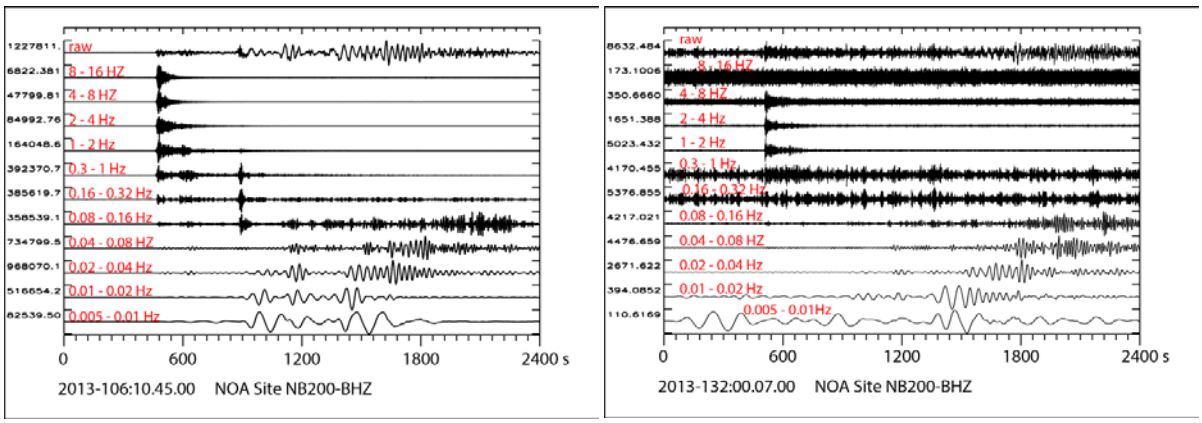

Fig. 6.2.14. Two earthquakes in Iran (left: 16 April 2013, 10:44:20 UTC, Mw 7.8; distance = 47.1°; right: 12 May 2013, 00:07:04 UTC, M 5.6; distance = 46.3°). All traces are normalized with their maximum amplitudes. The top traces are the raw data as recorded with the new CMG-3T Hybrid sensors. The other traces show in different frequency ranges Butterworth bandpass filtered data.

Fk-analysis results of the first P-wave onsets of these two earthquakes are shown in Figure 6.2.15 and the numerical values are listed in Table 6.2.3. The results shown for the 12 May 2013 event (Figure 6.2.15a and Figure 6.2.15b) show that application of the known time corrections improve the fk-analysis results in the typical frequency range of short period P waves: the data coherency becomes larger, the estimated backazimuth and apparent velocities are closer to the theoretically expected values and the number of side lobes is drastically reduced.

For the larger 16 April 2013 event the P-wave onset has significant amplitudes also at much lower frequencies (see Figure 6.2.14) and for the fk-analysis a much larger frequency range (here 0.08 – 4 Hz) can be utilized. The results are shown in Figures 6.2.15c and 6.2.15d. A comparison of the theoretical with the estimated values for backazimuth and apparent velocity show again a slight improvement after applying the time corrections, but the signal coherency decrease and the side lobes become more pronounced. This discrepancy can be explained as follows: The time corrections for NOA were developed for the large short-period NAO array in the 1970s. They empirically correct for lateral velocities below the array for signals with dominant frequencies between about 1 and 5 Hz. If it now becomes possible to analyze P-wave signals for much lower dominant frequencies (i.e., much larger wavelengths), the signals are dominantly influenced by lateral velocity heterogeneities in much larger volumes. In conclusion, the time corrections are signal frequency dependent and new empirical time corrections should be determined for utilizing the full possible frequency range for array studies.

Table 6.2.3: Fk-analysis results for the two Iran events.

Event	Figure	Frequency Band [Hz]	Backazimuth [deg]		App. Velocity [km/s]		Signal Coherence	Time Corrected
			Theory	Observed	Theory	Observed		
12/05/2013	15 a	1 – 4	116.77	118.01	14.15	13.76	0.26	no
12/05/2013	15 b	1 – 4	116.77	115.01	14.15	14.19	0.51	yes
16/04/2013	15 c	0.08 – 4	110.68	114.82	14.29	14.62	0.43	no
16/04/2013	15 d	0.08 – 4	110.68	108.34	14.29	14.60	0.38	yes

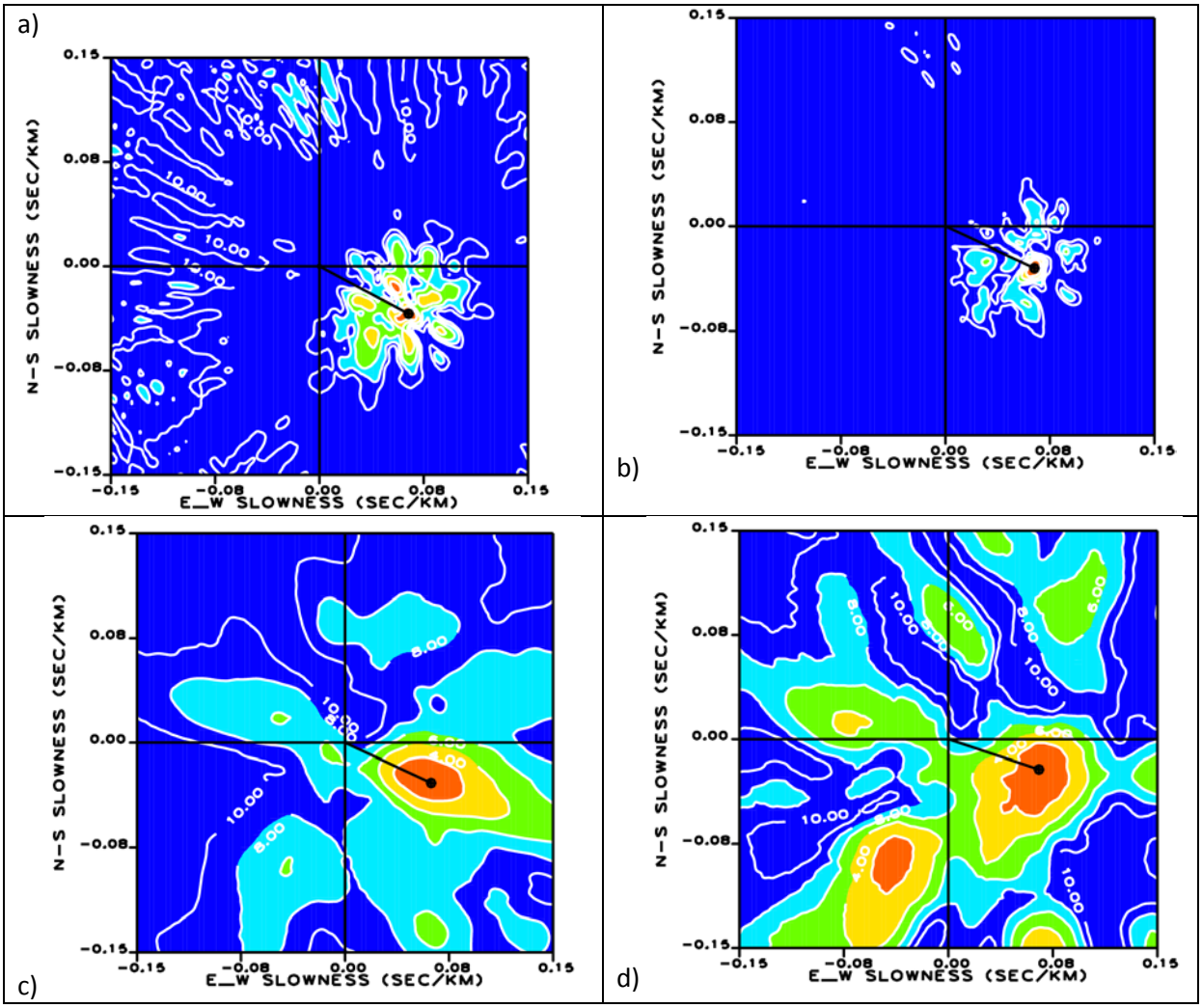

Fig. 6.2.15. Fk-analysis results for the two Iranian earthquakes: a) and b) for the 12 May 2013 event and c) and d) for the 16 April 2013event. NOA time corrections were applied for the results on the right (b and d).

M. Roth
J. Schweitzer
J. Fyen

References

Pirli, M. (2013). NORSAR System responses manual, 3rd Edition, NORSAR, 304 pp. + 5 Appendices.

Roth, M., J. Fyen, P. W. Larsen and J. Schweitzer (2011). Test of new hybrid seismometers at NORSAR, NORSAR Sci. Rep. **1-2011**, 61-71.

6.3 Reflectivity versus ray-tracing in infrasound propagation modelling

6.3.1 Abstract

This work considers infrasound propagation modelling. We compare results obtained using a classical ray-tracing program with results produced by the reflectivity method. The reflectivity method is applied widely by the seismological community to generate synthetic seismograms for elastic waves propagating in a stratified earth. However, to the best of the authors' knowledge, there has not been any previous comparison between ray-tracing and the reflectivity method for modelling the propagation of observed infrasound signals.

We apply a ray-tracing engine and a reflectivity code to the atmospheric conditions along the great circle path which connects the Drevja accidental explosion on December 17, 2013 and the IS37 infrasound array station near Bardufoss, Troms, Norway. The modelling results are compared with the observed signals recorded at the array.

6.3.2 Background

On December 17, 2013, a truck with 15 tons of slurry, to be used for road construction, exploded near the settlement of Drevja in the Nordland region of Norway. This event was considered also in Näsholm (2014). The origin time is estimated from local eyewitnesses to be 2013-351:14.26 and the coordinates are 65.988°N, 13.343°E. Signals from this event were observed at all of the Nordic infrasound arrays, and propagation paths to different stations observing the event are shown in Figure 6.3.1. The signals considered in the current work are recorded at the IS37 array which is situated around 410 km from Drevja.

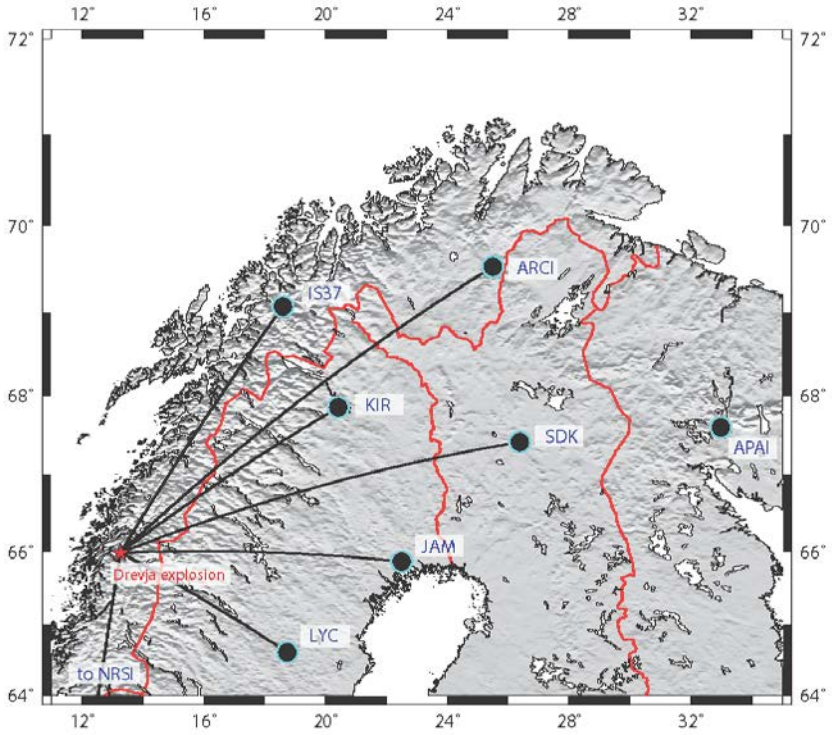

Fig. 6.3.1 Location of the Drevja accidental explosion in relation to infrasound arrays in the region.

6.3.3 Atmospheric model

The sound speed and winds applied from 0 to 75 km altitude are the GEOS5/MERRA public profiles published by NASA. Above this altitude, the profiles are compiled from the empirical NRLMSISE-00 (temperature) and HWM07 (wind) empirical models. The profiles at the location of the event and at the IS37 array are shown in Figure 6.3.2.

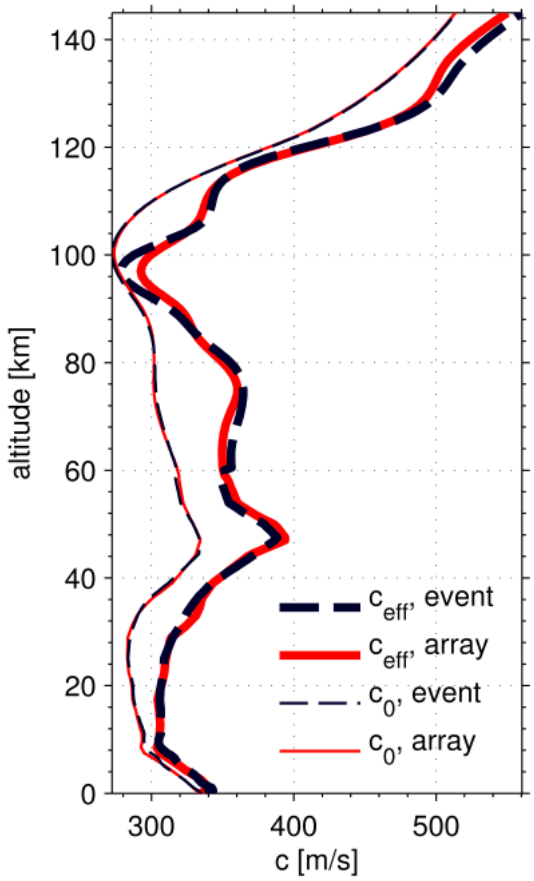

Fig. 6.3.2
Adiabatic sound speed as well as effective sound speed profiles at the event and at the IS37 array

6.3.4 Modelling approaches

We compare the following 4 modelling approaches for propagation of signals from Drevja to the IS37 array:

(A.) **ART2D ray-tracing with separated temperature and wind effects**
Ray-tracing using the ART2D code, while taking full advantage of its possibility to take wind effects into account separately from the sound speed. The sound speed is modeled in an anisotropic manner.

(B.) **Range-independent ART2D ray-tracing with separated temperature and wind effects**
Ray-tracing using the ART2D code, while taking full advantage of its possibility to take wind effects into account as in (A). However this approach incorporates no range-dependence of the atmosphere. The profile above the event is applied along the whole great circle.

(C.) **Range-independent, $c_{effective}$ ART2D ray-tracing**
Ray-tracing using the ART2D code, with range-independent atmospheric specifications (as in (B)). However, in this approach, wind effects are included only by constructing an effective speed of sound $c_{effective} \equiv c_0 + c_w$, where c_0 is the adiabatic temperature-dependent speed and c_w is the

projection of the wind speed in the direction along the great circle between the event and the array. The atmospheric model along the great circle is hence both range-independent and equal for any elevation angle in the propagation direction.

(D.) **Range-independent, $c_{effective}$ reflectivity modelling**

Application of the full waveform modelling reflectivity method (Müller, 1985) for a pulse within the same range-independent $c_{effective}$ medium as in method (C). In gas, only one type of elastic waves can propagate: the compressional wave. This purely acoustic wave propagation can be modelled simplistically with a pure SH-wave propagation code, but using the compressional wave velocities and the density of the atmosphere as the propagation model. For this application, the geometry of the original SH-code of G. Müller has been modified by letting the atmosphere be the modelled medium and the solid Earth correspond to the upper half-space in the original code. Also, the Earth-flattening approximation is adjusted to take a spherical atmosphere into account. The absolute amplitudes resulting from this modelling cannot be used since the code was written for displacements and the observations are pressure changes. However, the relative amplitude changes of the different phases should be correct. Figures 6.3.3, 6.3.4 and 6.3.5 illustrate the modelling results using ray-tracing approaches (A) – (C). Figure 6.3.6 illustrates the modelling arrival ground hit times using ray-tracing approaches (A) – (C) in comparison with the traces generated by the reflectivity method.

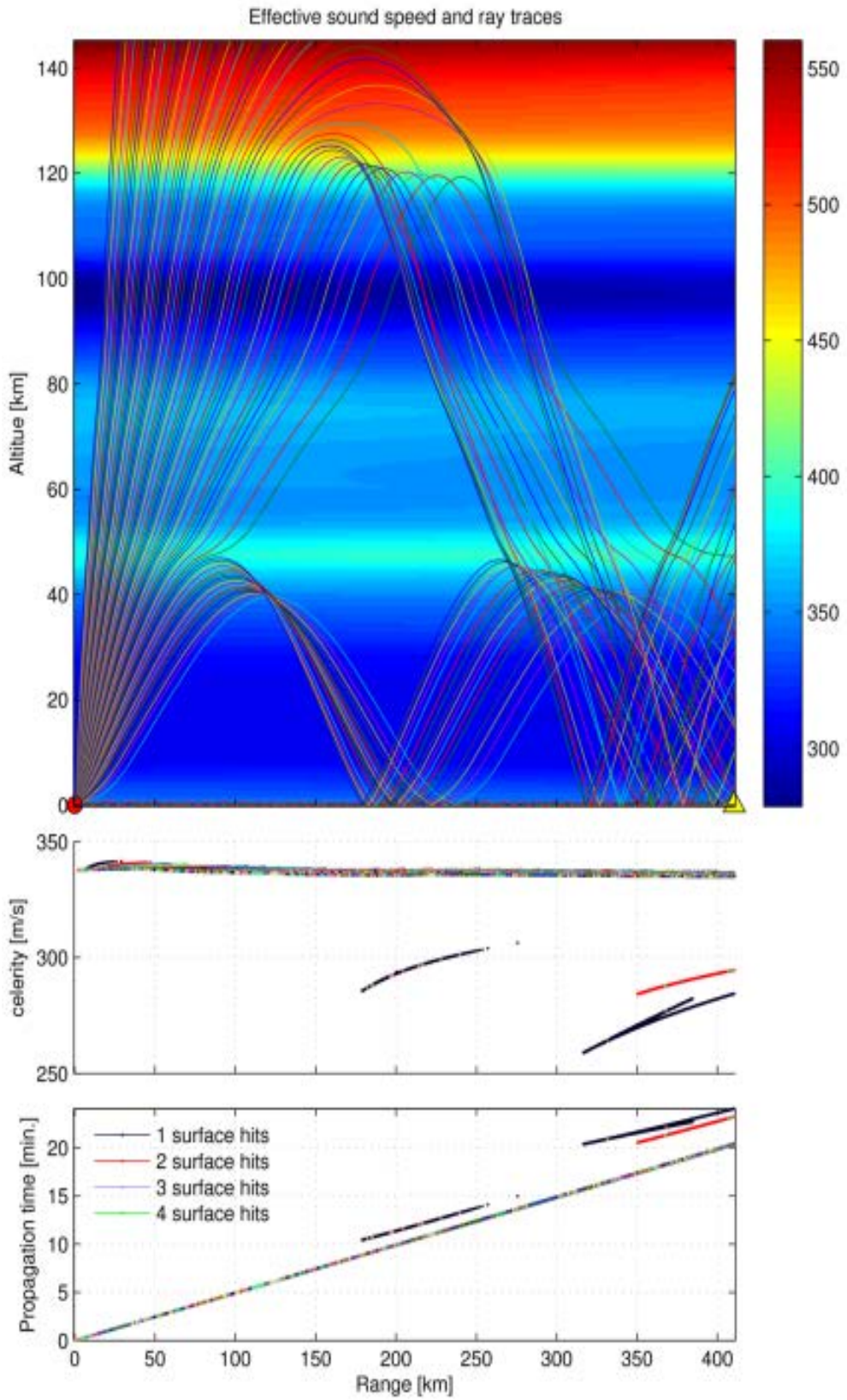

Fig. 6.3.3. Ray-tracing results using approach (A): ART2D ray-tracing with separated temperature and wind effects.

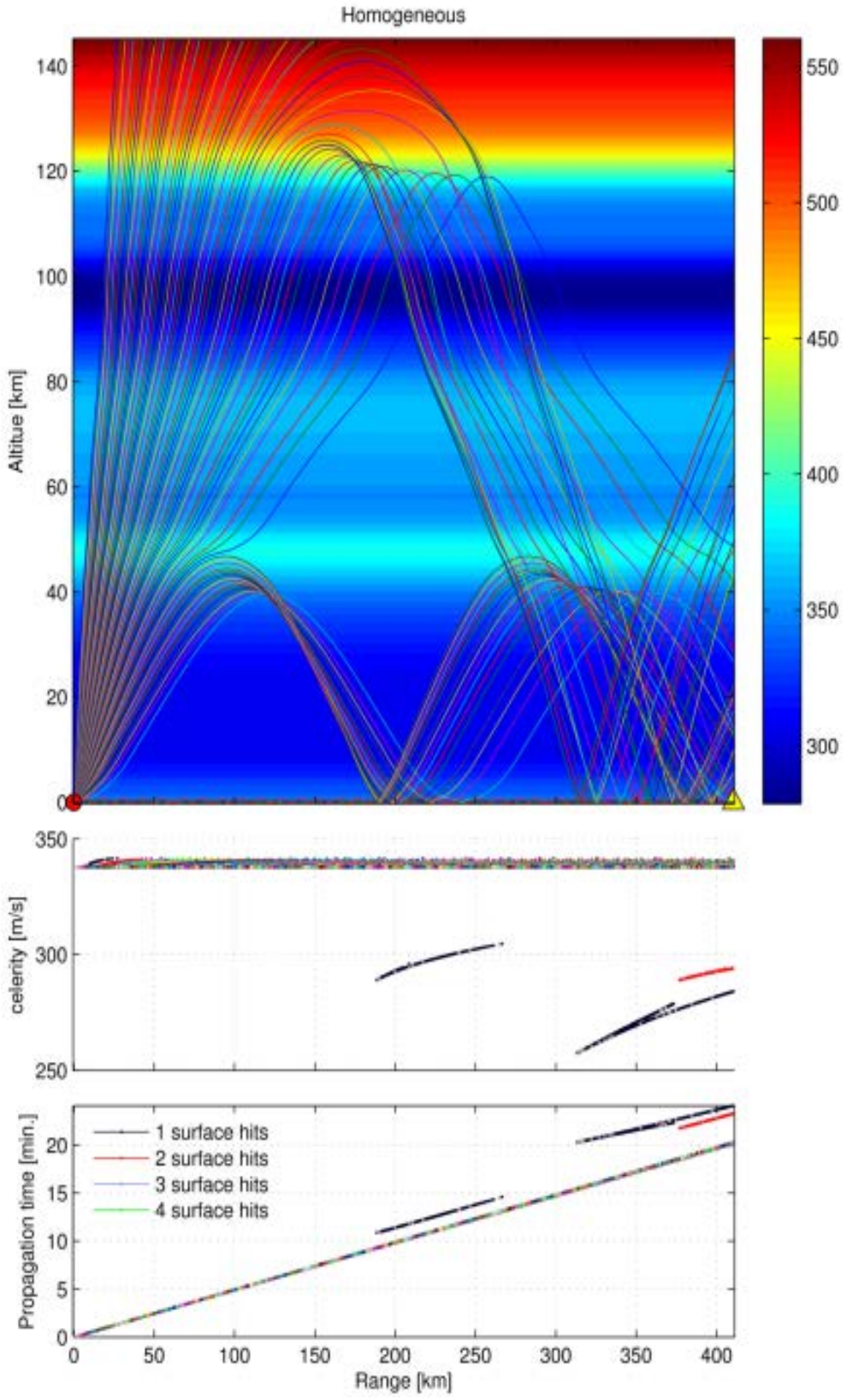

Fig. 6.3.4. Ray-tracing results using approach (B): Range-independent ART2D ray-tracing with separated temperature and wind effects.

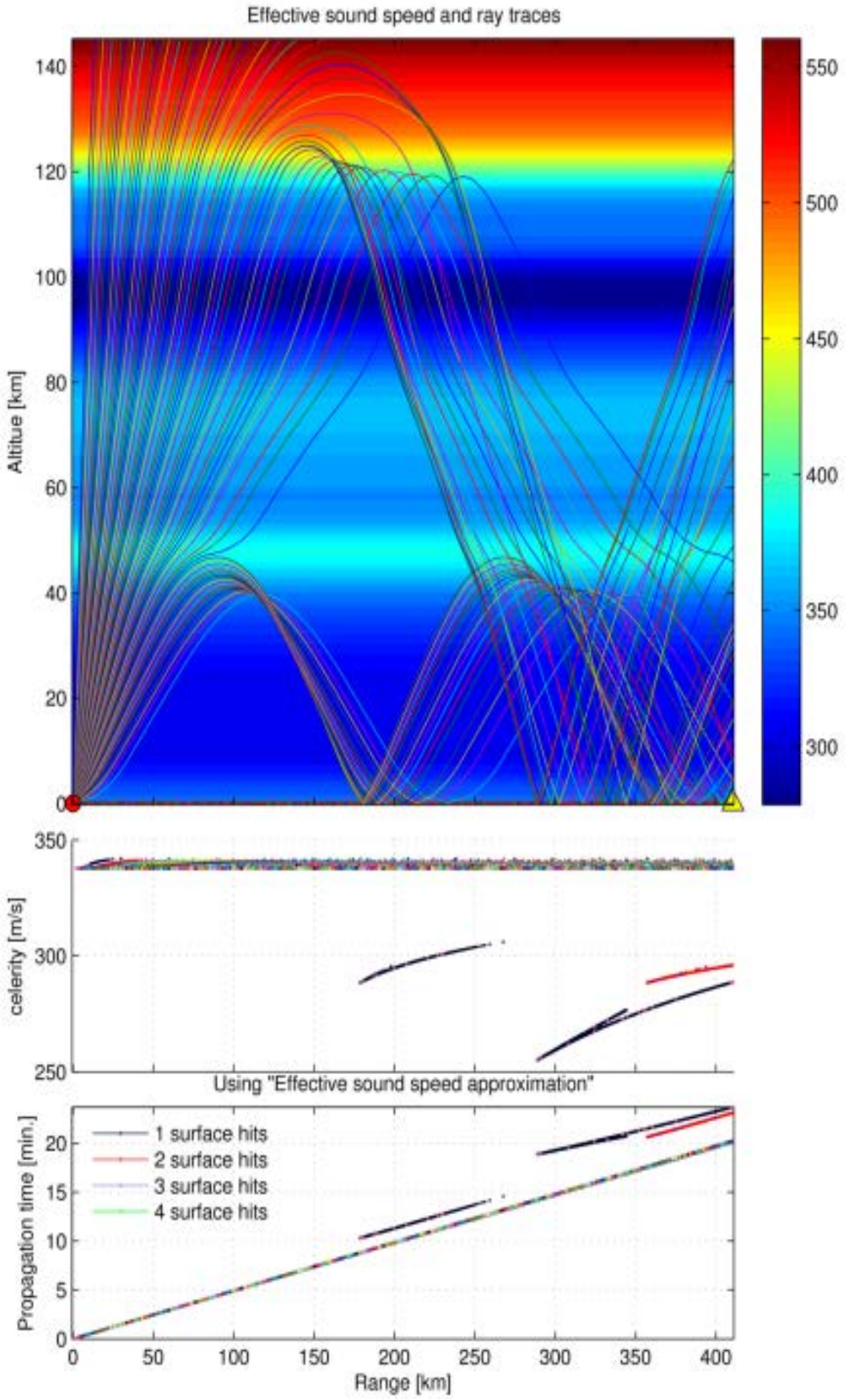

Fig. 6.3.5. Ray-tracing results using approach (C): Range-independent, $c_{effective}$ ART2D ray-tracing where wind effects are accounted for using the $c_{effective}$ approach

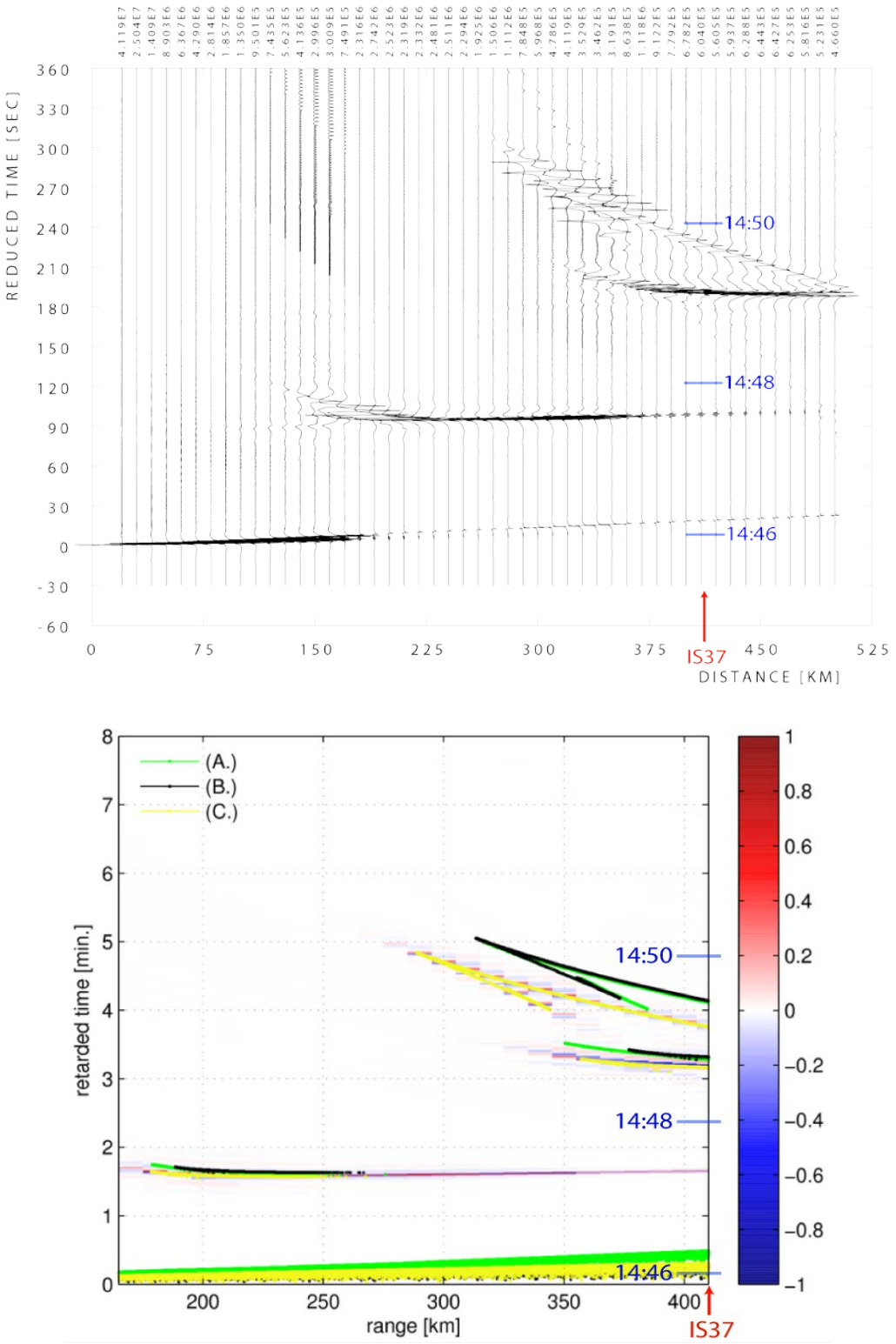

Fig. 6.3.6. Top panel: Signal traces generated by the reflectivity method. The reduced time velocity is 0.343 km/s. The signal dominant frequency is 2 Hz, while the calculation frequency range is 0.1 – 4 Hz sampled at 20 Hz. Each trace is normalized by a factor displayed in the top row. Bottom panel: The ray-tracing ground hit times from method (A), (B), and (C) overlaid on the color-coded amplitudes generated by the reflectivity method (D). The sensor array is located at a range of 410 km, as indicated by red arrows. The blue lines indicate the UTC times 14:46, 14:48, and 14:50 at the range of IS37.

6.3.5 Observed infrasound signals compared with modelling results

Figure 6.3.7 illustrates the signals recorded on the 10 sensors of IS37 in the frequency band 1-6 Hz. The high-frequency content of these signals, having propagated a distance over land of over 400 km, is significant. The signal-to-noise ratio (SNR) below 2 Hz is very low, and is far superior in the 2-5 Hz band. Such events demonstrate how useful the geometrical design of the array is with the innermost ring of closely spaced elements which allow the direction and apparent velocity of high frequency signals to be estimated.

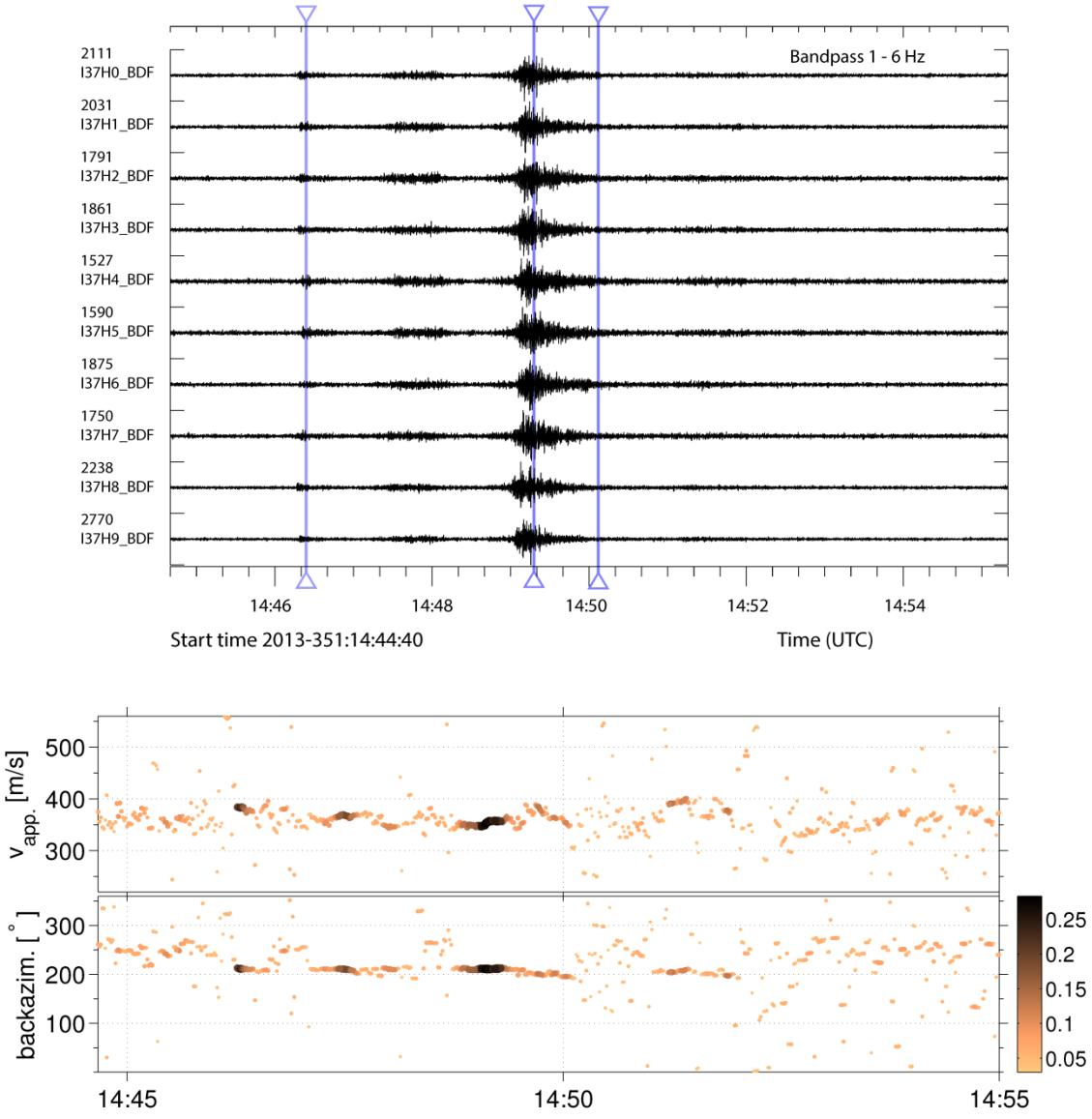

Fig. 6.3.7. Top panel: Waveforms recorded at IS37 with phase arrivals estimated by ART2D ray-tracing (approach A – Figure 6.3.3) indicated by blue vertical lines. Bottom panel: The corresponding apparent velocity and back-azimuth from f-k analysis.

6.3.6 Discussion

Observed tropospheric and stratospheric phases predicted by ray-tracing and reflectivity

The full ray-tracing (approach A – Figure 6.3.3) predicts three distinct infrasound phase arrivals at ground level at the IS37 array range: first a tropospheric arrival (at ~14:46 UTC), then a stratospheric arrival (at ~14:40.30), and finally a thermospheric arrival (at ~14:49.30).

The reflectivity modelling (Figure 6.3.6) predicts these tropospheric, stratospheric, and thermospheric arrivals. Also, an additional stratospheric arrival is present in the modelled traces, as discussed in the next subsection.

Looking at the observed waveforms in Figure 6.3.7, where the phase arrivals estimated by ray-tracing are indicated by vertical lines, we note that the first ray-tracing arrival estimate agrees with a received low-amplitude signal. The corresponding apparent velocity and back-azimuth from f-k analysis (shown below the waveforms) suggests that this is a tropospheric or stratospheric arrival from the direction of the event. Similarly, the second predicted ray-tracing arrival corresponds well with an observed high-amplitude signal.

Observed stratospheric phase predicted by reflectivity but not by ray-tracing

The data also reveal a phase arrival at around 14h47. This phase is not predicted by the ray-tracing procedure, but is anticipated by the reflectivity method as illustrated in Figure 6.3.6 (the phase arriving at the 410 km range at around 90s in reduced time). On the other hand, we see that the "first-bounce" arrivals predicted by ray-tracing within the approximate range interval [175, 275] km coincide with ones predicted by the reflectivity method (D). If we now in Figure 6.3.6 "extrapolate" these ray-tracing predictions all the way to the array location, we see that we are in line with both the reflectivity method predicted phase arrival and the phase observed in the collected data. Ray-trace modelling methods cannot predict such *head wave* phenomena.

Thermospheric phases

A thermospheric arrival is predicted by both the ray-tracing and the reflectivity modelling. But the arrival times of these predictions does not correspond with a signal visible in the data traces, nor with an increase in coherence between the elements.

However, looking at Figure 6.3.7 later in the data (at around 14:52 UTC), we can see a (very) slight "stabilization" of the backazimuth and apparent velocity estimates which might indicate the arrival of a weak thermospheric signal at the array.

Range-independence and $c_{effective}$ approximations

Figure 6.3.6 also illustrates that the ray-tracing methods (A) and (B) in this example provide very similar phase arrival times, hence indicating that the range-independent assumption is appropriate for modelling Drevja signal arrivals at IS37. On the other hand, the thermospheric and stratospheric phase arrival times predicted by ray-tracing with condition prescribed for approach (C) differ from the ones predicted by ray-tracing with the conditions prescribed for approaches (A) and (B), most significantly for the thermospheric arrivals. This is in line with the assumption that the greater the vertical portion of the ray propagation path is, the more the $c_{\text{effective}}$ assumption should deviate from

the true wind speed influence, which has to be taken in the true direction of propagation. The ray-tracing approach (C) uses the same range-independent $c_{effective}$ assumption as the reflectivity method (D). It is therefore intuitive that the phase arrivals predicted using (C) coincide with high pulse amplitudes calculated using (D).

6.3.7 Concluding remarks

By applying reflectivity modelling, we can avoid some limitations of conventional ray-tracing, e.g., we can get better head wave representation and less pronounced shadow zones. This is illustrated in our Drevja explosion example: the reflectivity method predicts a phase arriving at the station after turning only once in the stratosphere while ray-tracing does not predict this phase (which is observed in the recorded signals).

There are seismic modelling codes which model anisotropic velocity, and we intend to test these out for infrasound propagation. We foresee to more accurately model wind effects, hence avoiding disadvantages appearing due to the $c_{effective}$ approximation that we had to apply in the reflectivity modelling described in the current work.

References

Müller, G. (1985). The reflectivity method: a tutorial. J. Geophysics **58**, 153-174.

Näsholm, S.P (2014). Infrasound signal detection from the Drevja accidental explosion, Chapter 6.2, NORSAR Scientific Report **2-2013**, Semiannual Technical Summary, 1 July – 31 December 2013, (ed. Tormod Kværna), pp. 40-50.

Walker K. (2012). Atmospheric ray tracer 2D (ART2D). See the URL http://sail.ucsd.edu/~walker/software/ART2D/art2d.html

S. P. Näsholm, NORSAR
J. Schweitzer, NORSAR
T. Kværna, NORSAR
S. J. Gibbons, NORSAR